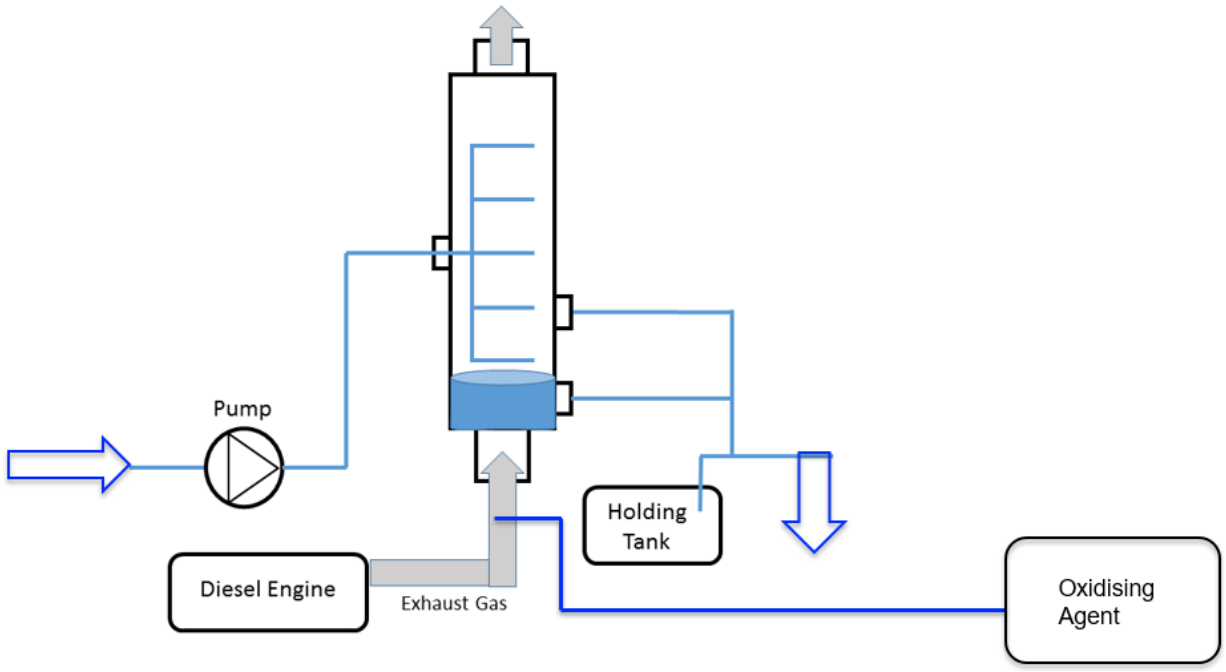
CHALMERS
UNIVERSITY OF TECHNOLOGY



Process evaluation of a SO_x and NO_x exhaust gas cleaning concept for marine application

SERWAH IBRAHIM

Department of Energy and Environment
CHALMERS UNIVERSITY OF TECHNOLOGY
Gothenburg, Sweden 2016

Master of Science Thesis 2016:09

Process evaluation of a SO_x and NO_x exhaust gas cleaning concept for marine application

SERWAH IBRAHIM



CHALMERS
UNIVERSITY OF TECHNOLOGY

Department of Energy and Environment
Division of Energy Technology
Chalmers University of Technology
Gothenburg, Sweden 2016

Process evaluation of a SO_x and NO_xx exhaust gas cleaning concept for marine application
SERWAH IBRAHIM

© SERWAH IBRAHIM, 2016.

Supervisor: Sima Ajdari, Energy and Environment
Supervisor: Shyam Bahadur Thapa, Yara Marine Technology
Examiner: Fredrik Normann, Energy and Environment

Master of Science Thesis 2016:09
Department of Energy and Environment
Division of Energy Technology
Chalmers University of Technology
SE-412 96 Gothenburg
Telephone +46 31 772 1000

Cover: Open loop process flowsheet.

Typeset in LaTeX
Printed by [Name of printing company]
Gothenburg, Sweden 2016

Process evaluation of a SO_x and NOx exhaust gas cleaning concept
for marine application
SERWAH IBRAHIM
Department of Energy and Environment
Chalmers University of Technology

Abstract

Maritime transport accounts for about 80% of all commercial cargo transport. The maritime sector is a large emitter of greenhouse gases, sulphur oxides, and nitrogen oxides. Since 1997, the International Maritime Organisation (IMO) set regulations (Marpol Annex VI) requiring maritime transport vessels to reduce exhaust emissions. Today vessels are required to fulfil stringent emission targets for SO_2 (Regulation 14 in Annex VI) and for NO_x (Regulation 13). A common method of reducing SO_2 emissions is by absorption of exhaust gases derived from the marine diesel engine, through wet scrubbing while NO_x is commonly reduced by SCR. Studies have shown that, under certain pH conditions and exhaust gas compositions, SO_2 and NO_2 can react in liquid phase to form stable compounds The objective of this work is to investigate a process for simultaneous absorption of SO_2 and NO_2. A steady-state simulation model is constructed in Aspen Plus, of a scrubber developed by Yara Marine Technology, which utilises the surrounding seawater in order to efficiently scrub SO_2 from exhaust gases. The simulation was performed in a packed RateSep model, with two configurations: one open loop (once-through liquid stream) model, and one closed loop (recycled liquid stream) model. Parameter data from a real life case is used to construct the model, and operational data from the absorber is used to verify the model. The results show that the process removes NO_x efficiently from the flue gas stream. There is also an overall improvement of the SO_2 removal compared to today's process. In open loop configuration, the formation nitrogen and sulphur is mainly bound as HADS. In the closed loop configuration, due to the recirculation, there is a risk of N2O formation that must be considered. The oxidation of the NO present in the flue gas requires an oxidizing agent. The process would requires around 119 kg ClO_2/h or 180 kg H_2O_2/h in order to oxidise all NO. In summary, there is a potential in utilising oxidation of NO to NO_2 combined with wet scrubbing in order to meet maritime regulations for both SO_2 and NO_x emissions, which can compete with the current combination of SCR and wet SO_2 scrubbing.

Keywords: Absorption, Maritime, SO_x, NO_x, pH, Exhaust Gas Treatment

Acknowledgements

I would firstly like to thank my examiner, Fredrik Normann, and my supervisor, Sima Ajdari, from Energy and Environment, Chalmers University of Technology, for all of their help with my thesis, for sharing their knowledge with me, and for their invaluable support during the course of the work. Thanks to Sima Ajdari for all of the help regarding Aspen Plus. Also, thanks to Yara Marine Technology in Norway, Oslo, and my supervisor Shyam Bahadur Thapa for the help and the access to information.

Serwah Ibrahim, Gothenburg, 2016

Nomenclature

Formula	Description
H_2O	Hydrogen Oxide
H^+	Hydrogen Ion
OH^-	Hydroxide Ion
$MgOH_2$	Magnesium Hydroxide
Mg^+	Magnesium Ion
CO_2	Carbon Dioxide
HCO_3^-	Bicarbonate
CO_3^{2-}	Carbonate
N_2	Nitrogen Gas
NO	Nitrogen Oxide
NO_2	Nitrogen Dioxide
HNO_2	Nitrous Acid
HNO_3	Nitric Acid
N_2O	Nitrous Oxide
NO_2^-	Nitrite
NO_3^-	Nitrate
SO_2	Sulphur Dioxide
HSO_3^-	Bisulfite
SO_3^{2-}	Sulfite
SO_4^{2-}	Sulfate
HADS ($HON(SO_3)_2^{2-}$)	Hydroxylamine Disulfonic Acid

Symbol	Description
D	Diameter $[m]$
D_V	Average Droplet Diameter $[m]$
A_t	Cross-sectional Area $[m^2]$
h_p	Packed Height $[m]$
h_L	Liquid Hold-up $[m]$
a_p	Specific Surface Area $[m^2/m^3]$
a_w	Wetted Surface Area $[m^2]$
a^I	Interfacial Area $[m^2]$
k_V	Gas Mass Transport Coefficient
k_L	Liquid Mass Transport Coefficient
ε	Void Fraction
Re_V	Reynolds Number for Vapour
$Re_L^{'}$	Reynolds Number for Liquid
Fr_L	Froude Number for Liquid
Sc_L	Schmidt Number for Liquid
Sc_V	Schmidt Number for Vapour

Abbreviation	Description
IMO	International Maritime Organisation
MARPOL	Marine Pollution (International Convention for the Prevention of Pollution from Ships)
MAN	Maschinenfabrik Augsburg-Nürnberg
ECA	Emission Controlled Area
SCR	Selective Catalytic Reduction

Contents

1 Introduction **1**
1.1 Background . . . 1
1.2 Purpose . . . 2

2 Background **3**
2.1 Maritime Emission Regulations . . . 3
2.2 Existing SO_2 Abatement Methods . . . 4
2.2.1 Maritime Scrubbers . . . 6
2.3 Existing NO_x Abatement Methods . . . 7
2.3.1 SCR . . . 7
2.4 Combined SO_2 and NO_x Abatement Technologies . . . 7

3 Case Study Review **9**
3.1 Green Tech Marine Scrubber . . . 9
3.2 Operational Data of Green Tech Marine Scrubber Case Study . . . 11

4 Theory **13**
4.1 Gas-phase Conversion of NO to NO_2 by Oxidisation . . . 13
4.1.1 Oxidising Agent: H_2O_2 . . . 13
4.1.2 Oxidising Agent: ClO_2 . . . 13
4.2 Absorption Chemistry . . . 14
4.2.1 Absorption of SO_2 . . . 14
4.2.2 Absorption of NO_x . . . 15
4.2.3 Nitrogen and Sulphur Interactions . . . 16
4.3 Mass Transfer . . . 17

5 Method **21**
5.1 Case Study . . . 21
5.1.1 Exhaust Gas and Seawater Composition . . . 21
5.2 Process Simulation . . . 22
5.2.1 Flowsheeting . . . 22
5.2.2 Validation Method . . . 24
5.2.3 RateSep Modelling . . . 24
5.2.3.1 Rate-Based Modelling . . . 25
5.3 Liquid-phase Chemistry . . . 27
5.3.1 Rate-controlled reactions . . . 27
5.3.2 Equilibrium reactions . . . 27

6 Validation **31**
6.1 Results 31

7 Evaluation of the Combined NO_x/SO_2 system **35**
7.1 Evaluation of Open Loop Operational Mode 35
7.1.1 Evaluation of liquid flow rate and removal efficiency 35
7.1.1.1 Reaction profiles 36
7.1.2 Evaluation of scrubber height and removal efficiency 37
7.2 Evaluation of the Closed Loop Operational Mode 38
7.2.1 Evaluation of liquid flow rate and removal efficiency 38
7.2.2 Reaction Profiles 39
7.2.3 Evaluation of scrubber height 40
7.3 Choice of oxidant: converting NO to NO_2 41
7.3.1 H_2O_2 as an oxidising agent 41
7.3.2 ClO_2 as an oxidising agent 42
7.3.3 Integration of oxidant into the system 42

8 Conclusion **43**

9 Further Work **45**

A Appendix 1 **III**
A.1 Contact Surface in Spray Scrubber III
A.2 Validation III

1
Introduction

1.1 Background

Maritime transport is the most common and potentially the cheapest form of long distance cargo transport, about 80% of all world trade is made by water [1]. Large cargo ships or cruise ships commonly run on heavy fuel oil, which has a high sulphur content with an average of 2.7% [2]. Emissions derived from maritime transport consist mainly of carbon dioxide (CO_2), nitrogen oxides (NO_x), and sulphur oxides (SO_x), and studies made on marine pollution [3] indicate that the marine diesel engine is the largest atmospheric polluter of the two latter: nitrogen and Sulphur oxides. SO_x and NO_x pollution can have a great impact on the environment. SO_x is a large contributor the acid rain since SO_2 can oxidise to SO_3 to form H_2SO_3 (sulphuric acid) when in contact with water, and NO_x is involved in aiding the formation of ground level ozone and contributes to the depletion of the ozone layer [4].

Since 1997, the International Maritime Organisation (IMO) set regulations (Marpol Annex VI) requiring maritime transport vessels to reduce exhaust emissions [5]. In accordance to Regulation 14 in Annex VI, sulphur content in fuels is to be reduced to 0.1% for ECA (Emission Controlled Area) and 0.5% in international waters from 1 January 2015 [6]. Regulation 13 requires ships to reduce NO_x emissions and is divided in to three parts: Tier I, Tier II, and Tier III, where Tier III applies to recently (2016) constructed ships moving within North American waters [7]. Tier III requires manufacturers to install NO_x reducing process components, since a reduction of this magnitude is not possible by solely controlling the combustion process [8]. Regulating exhaust gas emissions from shipping has previously not existed [9], and there is therefore little experience in emission-reducing technologies relative to the industrial and energy sector.

There are several possible ways of meeting the requirements of Tier III and Regulation 14: this can be done either by switching to a low sulphur fuel or by exhaust after-treatment through absorption. Today, scrubbers focus solely on the absorption of SO_2, while NO_x is removed separately, often through catalytic reduction. There is therefore a potential in removing both NO_x and SO_2 through absorption in order to reduce costs.

Recent research on the simultaneous absorption of NO_2 and SO_2 from gas to liquid phase, under pressurised conditions, has provided more knowledge about the interactions between NO_2 and SO_2 [10] in liquid phase. Conditions, such as: flue gas composition, and specifically pH, have shown to have an effect on the reaction

pathways that occur in liquid phase [10] between nitrogenous and sulphuric compounds. By controlling these conditions, it is not only possible to efficiently absorb NO_2, but furthermore improve the absorption of SO_2. This knowledge is very applicable to seawater scrubber systems for marine application, and can have an effect on the dimensioning of the scrubber, and the consumption of seawater, and alkali chemicals. The focus on this study is to investigate the feasibility of simultaneous removal of NO_x and SO_2 through an absorption process developed by Yara Marine Technology. This work is performed through simulation of a real-life case of a SO_2 absorption process that is installed in a cruiser ship, using the simulation tool Aspen Plus. Data for this case is provided by Yara Marine Technology.

1.2 Purpose

This work is a case study of a spray-type hybrid absorption system, developed by Yara Marine Technology, the model of the system is constructed using the simulation and modelling tool Aspen Plus. The aim of the case study, is to investigate the feasibility of NO_x removal in a seawater SO_2 scrubber system, installed in a cruiser ship, and what effects the interactions that occur in the liquid phase between nitrogen and sulphur can have on the removal of SO_2. Furthermore, the work aims to review if there are possibilities of optimising the absorption process in terms of reducing the consumption of seawater, as well as the dimensioning of the scrubber, as a result of nitrogen and sulphur interactions.
This work is limited to only investigating the presented case study, the liquid phase chemistry between nitrogen and sulphur that occurs in the scrubber, as well as reviewing oxidants needed to oxidise NO to NO_2 in gas phase.

2

Background

2.1 Maritime Emission Regulations

SO_x emissions are restricted by MARPOL's Annex VI, Regulation 14 and applies to all fuel oils used in marine transportation [5]. Restrictions are based on the sulphur content in fuel oils and can be seen in Table 2.1:

Table 2.1: SO_x regulations according to Annex VI, Regulation 14, within and outside of Emission Control Areas (ECA) [5]. The limits express the mass percentage of sulphur content in the fuel (% mS/m_{fuel})

Outside ECA	Inside ECA
4.5% prior to Jan. 2012	1.5% prior to July 2010
3.5% Jan. 2012	1.0% July 2010
0.5% Jan. 2020	0.1% Jan. 2015

The location of the ECA (Emission Control Areas) are shown in Figure 2.1 which include: Baltic Sea area, North Sea area, North American area, United States Caribbean Sea area.



Figure 2.1: A map that highlights the areas that are classified as ECA, which is comprised of the Baltic Sea, North Sea, North American sea, and the Caribbean sea. Photo: Yara Marine Technology

However, Regulation 14 in Annex VI, allows for post-combustion measures such as scrubbing as an alternative way of complying with SO_x regulations. Furthermore, there are specific areas, often coastal, where discharge of treated washing water is not allowed [11]. For operating ships and marine engines exceeding 130 kW output, constructed on or after 2000, NO_x emissions are regulated by IMO's MARPOL 73/78 Annex VI, Regulation 13 [11].

Table 2.2: NO_x regulations according to Annex VI, Regulation 13. Tier III applies to North American emission control areas. [15]

Tier	Date	$\underline{gNO_x/kWh}$ $n < 130rpm$	$\underline{gNO_x/kWh}$ $n = 130 - 1999rpm$	$\underline{gNO_x/kWh}$ $n \geq 2000rpm$
I	1 Jan. 2000	17.0	$45n^{-0.2}$	9.8
II	1 Jan. 2011	14.4	$44n^{-0.23}$	7.7
III	1 Jan 2016	3.4	$9n^{-0.2}$	2.0

n = rated engine speed, rounds per minutes (rpm)

As seen in table 2.2, the restriction of NO_x is highly dependent on the type of engine and its rated speed. In most international waters, Tier II applies [15] for all large ships. Tier III is the most stringent method, and often external abatement measures are required apart from controlling the engine combustion process [8]. There are few proven and commercially available methods that can comply with Tier III regulations, two of these are SCR (Selective Catalytic Reduction) and LNG (Liquefied Natural Gas) [11].

2.2 Existing SO_2 Abatement Methods

In recent years, the application of absorbers for SO_2 removal has increased substantially in marine transport, and they are commonly called scrubbers. Scrubbers are classified as dry scrubbers, utilising dry lime and other calcium-based minerals for pH control, or classified as wet scrubbers that use an alkali liquid solution [11]. Currently, wet scrubbers dominate the marine industry. There are several reasons to why wet scrubbing applies well for marine application. One main reason is that absorption of SO_2 is a, comparatively, cheaper alternative than fuel desulphurisation [2], scrubber systems are easily retrofitted into older ships, and the scrubber system can be dimensioned so that it replaces the silencer [6]. There are several factors that affect the design of the scrubber system such as: fuel oil-type, engine size, allowable pressure drops, electrical consumption, and space restrictions, that are unique to a vessel. Since seawater is readily available, seawater consumption only becomes an issue if the weight of the scrubber succeeds weight restrictions.
The simplest scrubber system available is the open loop scrubber, where water is sourced from the surrounding sea, pumped through a filter and sprayed into the scrubber from the first top stages using nozzles that disperse water into droplets [11]. An open loop scrubber is only efficient if the source of water is alkaline. This can either be done by adding an alkali chemical or by utilising seawater, which has a natural alkalinity derived from the bicarbonate ion (HCO_3^-) present in the seawater.

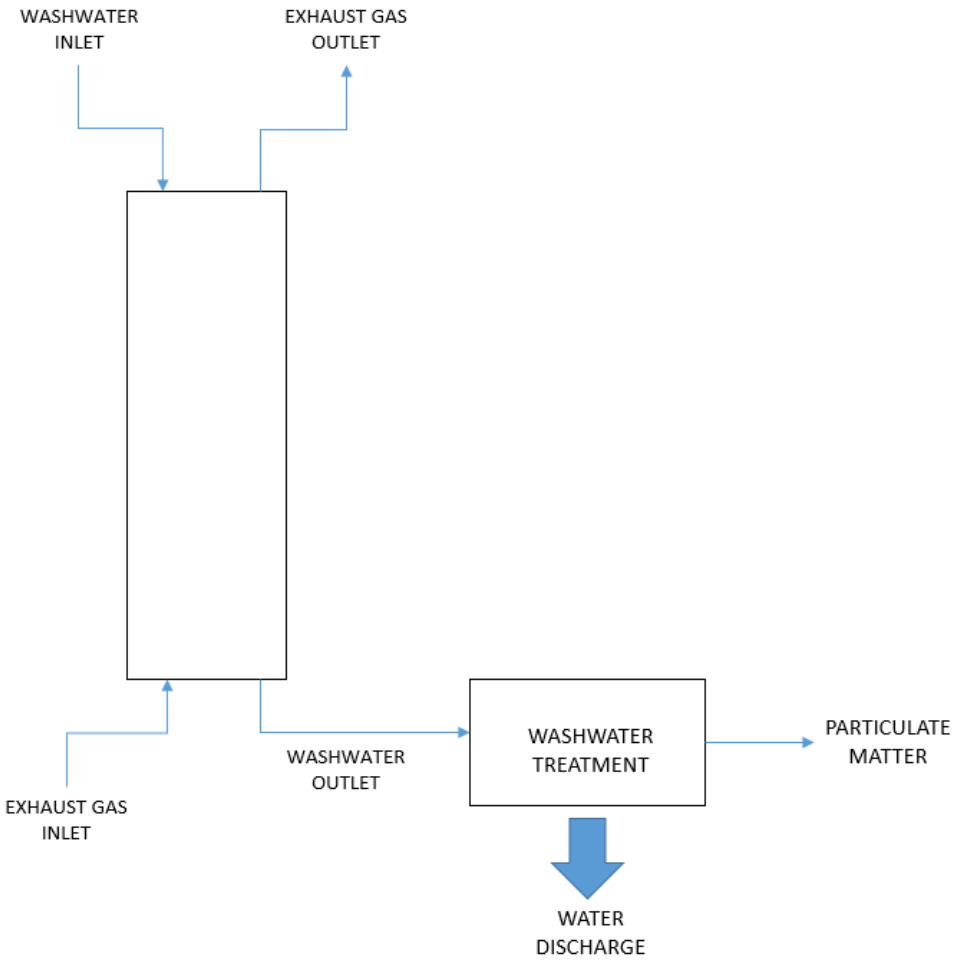


Figure 2.2: A schematic of a open-loop wet scrubber system. Water is sourced from the sea and sprayed over the exhaust gases. Particles are removed from the water and discharged back into its previous environment. [11]

The water is discharged back into the sea after particular matters are removed. This type of solid waste generated from scrubbing is classified as hazardous waste, and therefore stored and later handled at land [11]. Closed loop scrubber systems are developed for no-discharge zones, this requires that the scrubber system works on a recirculated flow that is later discharged as the vessel leaves a no-discharge area. Depending on the amount of water consumed and the size of the buffer tank, the closed loop system can only run for a certain amount of time until the liquid is saturated. Therefore, to avoid saturation and increase the time span, the liquid phase is continuously bleed off, adding more seawater into the system.

As SO_2 is being absorbed, the pH of the liquid decreases due to formation of sulfurous acid (H_2SO_3) and in order to increase the removal efficiency and to allow for more SO_2 to be absorbed, an alkali is added. It is most common to add sodium hydroxide (NaOH) [11] , but there are other alternatives available such as magnesium oxide (MgO).

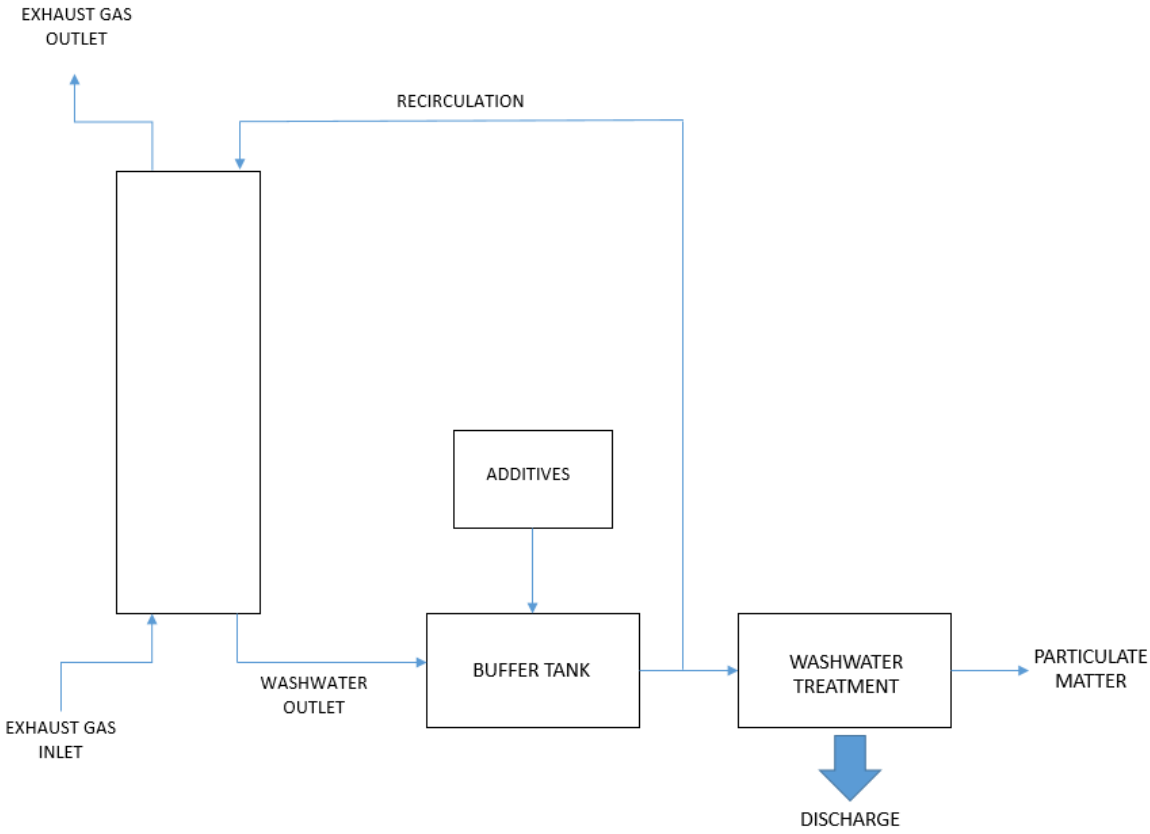


Figure 2.3: The closed-loop system requires water to be recirculated as the vessel enters a no-discharge zone. Through a buffer tank the water is bled off and stored until it can be discharged. The alkali is usually added though the buffer tank. [11]

2.2.1 Maritime Scrubbers

There are several types of maritime SO_2 scrubber systems that are commercially available today. Scrubbers come as either packed, spray-type or even turbo scrubbers. Furthermore, the scrubbers can also be of inline type, and this means that the exhaust gas pipe is connected directly to the scrubber. Table 2.3 lists the commercially available maritime scrubbers today and their SO_2 removal performance as well as their dimensioning.

Table 2.3: SO_2 Removal Technologies

Scrubber:	**Height[m]**	**Diameter[m]**	**SO_2**
PureteQ Maritime Turbo Scrubber* [12]	8.5-12.5	1.17-2.6	$> 98\%$
Wärtsila Inline Scrubber** [13]	10-12.5	1.85-3.25	$>98\%$

*Engine size: 2-15 MW **Engine size: 6-18 MW

The PureteQ turbo scrubber has a unique hydrodynamic distribution method that forces the liquid to move in a swiveling motion, which allows for fast quenching of SO_2 before scrubbing [12] as well as good gas and liquid contact. This method also

allows for the scrubber to be placed either vertically or horizontally. The Wärtsila inline scrubber is a vertical spray-type scrubber, where the liquid (seawater) is sprayed over the exhaust gases in a counter current exchange.

2.3 Existing NO_x Abatement Methods

2.3.1 SCR

Selective Catalytic Reduction (SCR) is a catalytic method of reducing the amount of NO_x, from exhaust gases, effectively by converting NO_x into N_2 and H_2O. Depending on the amount of NO_x present, the type of engine and catalyst, the reduction can vary between 70-95% [11].

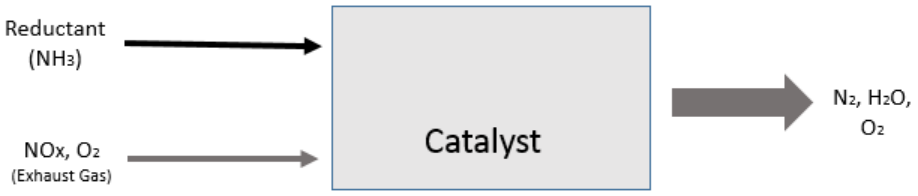


Figure 2.4: A principal sketch of the catalytic reduction of NO_x from exhaust gas, using ammonia as a reducing agent.

In the catalytic environment, a reducing agent is sprayed into the chamber and mixed with the exhaust gas. An example of a catalytic reaction is shown below, with ammonia (NH_3) as a reducing agent:

$$4NO + 4NH_3 + O_2 \rightarrow 4N_2 + 6H_2O \tag{2.1}$$

$$2NO_2 + 4NH_3 \rightarrow 3N_2 + 6H_2O \tag{2.2}$$

$$NO + NO_2 \rightarrow 2N_2 + 3H_2O \tag{2.3}$$

SCR is the most common way of tackling NO_x emissions in shipping for Tier III compliance, converting a toxic gaseous substance (NO_x) into harmless compounds. The catalyst is placed conveniently after the marine engine and takes up very little space [11]. However, these catalysts often use expensive metals as a catalytic surface (vanadium, copper etc.) which can deteriorate over time, this makes SCR a costly method for reducing NO_x emissions in marine exhaust gas [11].

2.4 Combined SO_2 and NO_x Abatement Technologies

In the shipping industry, the removal of NO_x and SO_2 from exhaust gases is commonly done separately and these methods, such as combining SO_2 scrubbing together

with SCR, are costly. Recently, simultaneous removal of both NO_x and SO_2 have been investigated due to its potential in reducing overall costs. The technology of combining NO_x and SO_x removal through wet scrubbing, for marine application, is not yet widely commercially available. There are scrubbers such as the Ecospec CSNOx Technology that reduces both SO_2, NO_x and CO_2 gases [14]. Overall the system consists of five main parts: seawater intake system, spray water system, abator tower system, wash water system, and exhaust gas monitoring system.

Table 2.4: The performance of the Ecospec CSNOx Technology system

	SO_x Removal	**NO_x Removal**	**CO_2 Removal**
CSNOx	99%	66 %	77 %

In industrial processes, such as coal-fired or oil-fired power plants, where the fuel is rich in sulphur, a technology for simultaneously removing both NO_x and SO_2 post-combustion has been growing in popularity and extensive research in this area is being made. Table 2.5 lists some technologies that are either in trial, and/or commercially available.

Table 2.5: Combined NO_x/SO_2 Removal Technologies in Industrial Processes

Technology:	**SO_x Removal**	**NO_x Removal**
Electron beam flue gas treatment [16]	≤98%	≤82 %
Wet scrubbing (using an aqueous $NaClO_2$) [17]	88–100%	36–72%
LoTOx™ (ozone injection and wet scrubber) [18]	>95%	90–95%
NeuStream®-MP (ozone oxidation) [18]	97%	>90%

A drawback of using a electron beam flue gas treatment, which is a non-thermal plasma technology, is the consumption of power [18]. LoTOx™ has a similar issue, since it utilises ozone generators in order to oxidise NO. NeuStream®-MP uses a similar oxidation process, but also includes CO_2 capture. In industrial processes, the availability of power is not as big of a problem as it is for ships that travel long distances in open waters. This becomes a problem when attempting to use these combined NO_x and SO_2 removal technologies.

3
Case Study Review

Yara Marine Technology, former Green Tech Marine, specialises in providing exhaust gas treatment solutions for maritime and offshore industries. This section reviews a case study of a Yara Marine Technology hybrid scrubber system, Green Tech Marine Scrubber, installed into a cruise ship. Not only can this scrubber system meet SO_x regulations, but the Green Tech Marine scrubber has the advantage of being amongst the smallest scrubbers commercially available [6].
The specifications for the cruise ship that is relevant to the study and the installed hybrid absorber can be seen below in table 3.1.

Table 3.1: Specifications of the cruise ship

Ship Type	Cruise Ship
Engine Model	Wärtsilä 12V46 (4stroke)
Engine Output	12.6 MW
Heavy Fuel Oil Consumption	200 kg/MWh
Maximum Gas Flow Rate	20 kg/s
Exhaust Gas Temperature	260 C
Absorber Dimensions:	
	2.3m diameter
	16m height (60% (9.6m) mass transfer surface)

Log data is available for when the absorber runs in both closed and open loop mode. The data includes: seawater flow rate, exhaust gas flow rate, sulphur composition in the exhaust gas, outgoing and ingoing pH levels, as well as the sulphur removal efficiency.

3.1 Green Tech Marine Scrubber

The hybrid scrubber system, can run in two operational modes: one open loop mode, and one closed loop mode. Figure 3.1 shows a schematic overview of the open loop configuration.
The scrubber is also called an inline scrubber, where the exhaust gas travels from the bottom, close to the engine, to the top without any form of bypassing. This means that scrubbers can be slimmed down to the extent that its dimensioning resembles that of an engine silencer. The seawater is sourced from the ballast tank,

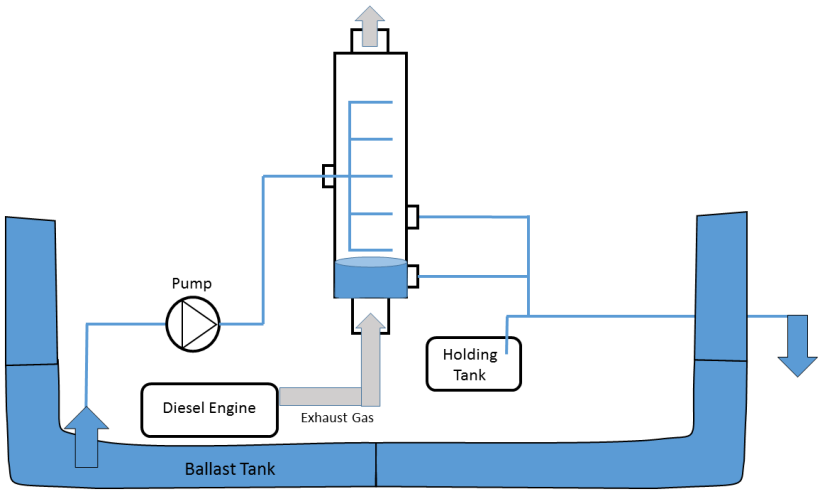


Figure 3.1: The Yara spray absorber, when operated in open loop. The absorber is also called an in-line scrubber, meaning that the exhaust gas travels vertically through the scrubber. Ballast water is pumped and sprayed over the exhaust gas from several levels along the scrubber.

and through nozzles that are placed along the scrubber in layers to ensure good mixing, the seawater is sprayed over the exhaust gas. A water trap is placed at the bottom of the scrubber, which hinders water from travelling back to the engine. The configuration for when the scrubber system operates in closed loop mode can be seen in figure 3.2.

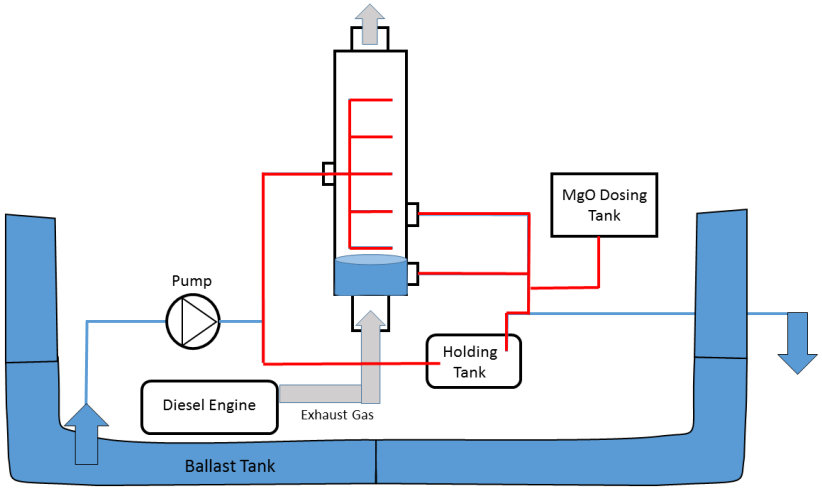


Figure 3.2: The recycle stream in the closed loop configuration is denoted by the red lines. Also, it can be seen that alkali (MgO) is added at the outlet scrubbing water, before the holding tank.

As figure 3.3 shows, the closed loop configuration is more complicated than a once-through open loop configuration. As scrubbing water leaves the scrubber, MgO is added, and a small portion of the liquid is bleed off. The water then flows into a

holding tank where the liquid is cleaned from particulate matter. The scrubbing water, and a small portion of make-up water sourced from the ballast tank, is cooled, using ballast water, before it re-enters the scrubber. By bleeding off and re-introducing small portions of fresh seawater into the system, the scrubber is able to operate in closed loop mode during longer periods than otherwise, this by avoiding a saturation of the liquid. In closed loop operation, the scrubbing water cannot be fully discharged into the surrounding waters due to regulations in the area. This means that the size of the holding tank, as well as the amount of consumed seawater, becomes an important factor and can affect how long the scrubber system can operate in closed loop mode.

3.2 Operational Data of Green Tech Marine Scrubber Case Study

The case study running data of the scrubber system describes the performance of the scrubber, both in open and closed loop operational mode, in terms of SO_2 removal efficiency. The running data from the open loop operational mode describes the performance as a function of liquid-to-gas ratio.

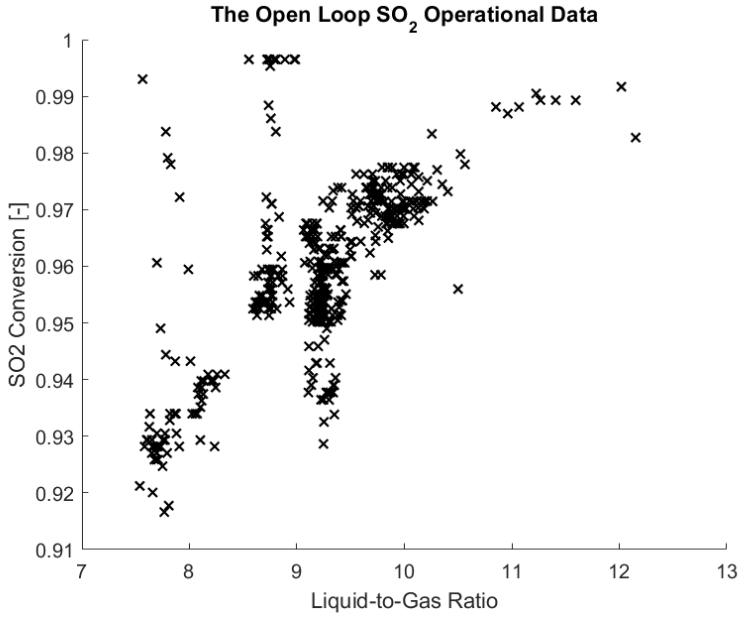


Figure 3.3: The figure shows that the removal efficiency increases as the liquid-to-gas ratio increases.

The open loop scrubber uses no alkali to control the absorption process, this means that the parameters that control the SO_2 removal efficiency is the exhaust gas flow and the seawater flow rate. The SO_2 removal efficiency in closed loop operational mode however is not only dependent on the exhaust gas rate and the seawater flow rate, but also the addition of alkali (MgO). Figure 3.4 illustrates the SO_2 removal efficiency as a function of liquid-to-gas ratio.

The figure (Figure 3.4) shows that overall the removal efficiency is high and that the liquid-to-gas ratio does not vary as much as for the open loop operational mode.

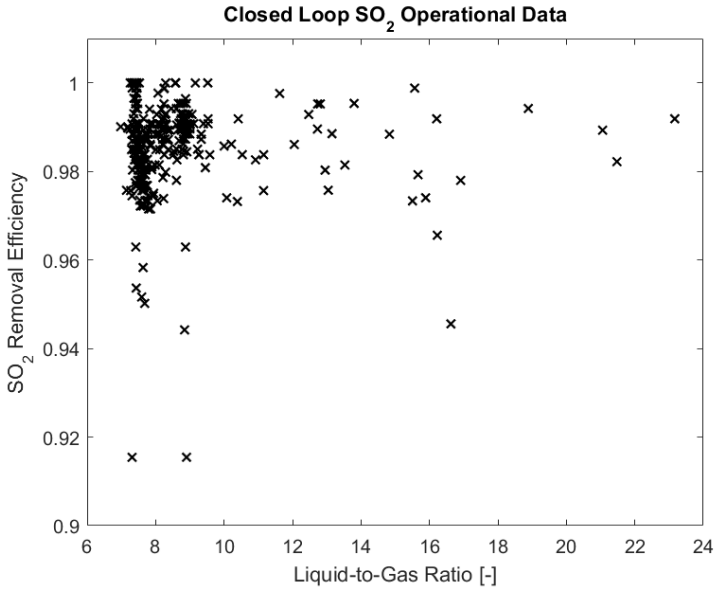


Figure 3.4: The running data over the scrubber system in closed loop operational mode.

Figure 3.5 shows (1) the effect of MgO dosing [$litres/min$] on the SO_2 removal efficiency, (2) how the MgO (magnesium oxide) dosing varies for different liquid-to-gas ratios. The figure (Figure 3.5) shows that there is no clear correlation between the removal of SO_2 and the MgO dosing, and that the MgO dosing is not clearly connected to different gas or liquid flow rates.

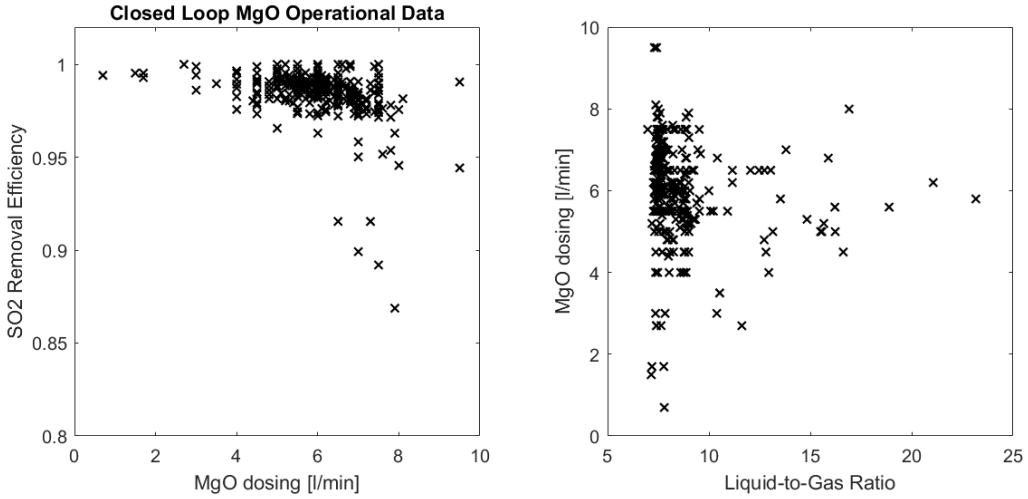


Figure 3.5: The log data shows that range of the MgO dosing and the SO_2 conversions.

4

Theory

This chapter presents the theory which constitutes the basis for this work. This mainly includes the liquid-phase and gas-phase chemistry, as well as a theoretical background on relevant mass transport theory.

4.1 Gas-phase Conversion of NO to NO_2 by Oxidisation

The combustion process favours the formation of NO over the formation of NO_2. Furthermore, NO has a low solubility and in order to achieve an efficient scrubbing, NO can be conveniently converted to NO_2 by injecting an oxidiser into the exhaust gas. There are several types of oxidisers that can be used, all with the possibility of fully oxidising all NO. In this work, H_2O_2 and ClO_2 are reviewed.

4.1.1 Oxidising Agent: H_2O_2

Hydrogen peroxide (H_2O_2) can be directly injected into a hot exhaust gas stream [19] and since the reaction is fast, it effectively converts NO into NO_2. The NO reacts directly with HO_2 radicals, that are created when H_2O_2 is thermally decomposed.

$$H_2O_2 \rightarrow 2OH \tag{4.1}$$

$$\cdot OH + H_2O_2 \rightarrow H_2O + HO_2 \tag{4.2}$$

The formation of HO_2 radicals allows for NO to easily convert into NO_2.

$$HO_2 + NO \rightarrow NO_2 + \cdot OH \tag{4.3}$$

The conversion of NO can occur rapidly in moderate temperatures and have been shown to be effective in temperatures around 600 K [19].

4.1.2 Oxidising Agent: ClO_2

Oxidisation of NO through addition of ClO_2 is, in gas phase, a rapid reaction. It has been shown that a stoichiometric addition of ClO_2 can rapidly oxidise up to 95%, occurring within 2 seconds [20].

$$NO + ClO_2 \rightarrow NO_2 + ClO \tag{4.4}$$
$$NO + ClO \rightarrow NO_2 + Cl \tag{4.5}$$

However, chlorine dioxide is hazardous and can harm the utility when scrubbing [20]. The chlorine ion can either form hydrogen chloride (HCl) in the presence of water, or can contribute to side reactions involving NO_2 and SO_2 that can complicate the wet scrubbing.

4.2 Absorption Chemistry

The absorption of a component i into the liquid phase is dependant on the solubility of the component, i.e. how well a component is dissolved into the liquid phase. Henry's law states that the amount of gas absorbed is proportional to the partial pressure of the component in the gas phase [21].

$$C_i = H_i p_i \tag{4.6}$$

where C_i [mol l^{-1}] expresses the concentration of component i in the liquid phase, p_i [bar] the partial pressure of component i in gas phase, and H_i is the Henry solubility constant [mol l^{-1} bar^{-1}]. Furthermore, the solubility constant H_i is specific for a component and can be derived from Henry's law:

$$H_i = \frac{C_i}{p_i} \tag{4.7}$$

When NO_x and SO_2 are absorbed into a water, new compounds, such as HNO_2, HSO_3^-, are formed, and these can interact with one and other in many pathways to form more complex compounds. In order to efficiently absorb both SO_2 and NO_x, the interactions that occur in the liquid phase are important to understand.

4.2.1 Absorption of SO_2

In a heterogeneous liquid-gas system, gas-phase SO_2 and liquid-phase S(IV) (HSO_3^-, $SO_2 \cdot H_2O$, SO_3^{2-1}) is assumed to be in equilibrium [22], and can be expressed by equilibrium reactions, which are shown below. Firstly, the gaseous SO_2 is absorbed into the liquid phase:

$$SO_2(g) + H_2O \rightleftharpoons SO_2 \cdot H_2O \tag{4.8}$$

The absorption of SO_2 (g) into liquid phase is dependant on the solubility of SO_2 in water and the Henry constant (H_{SO_2})

$$H_{SO_2} = [SO_2 \cdot H_2O]/p_{SO_2} \tag{4.9}$$

H_{SO_2} is the Henry solubility constant for SO_2, p_i the partial pressure, and [$SO_2 \cdot H_2O$] [mol l^{-1}] is the concentration of SO_2 in liquid phase. Liquid phase sulphur dioxide will further react to water and form bisulfite: an acidic compound.

$$SO_2(aq) + \cdot H_2O \rightleftharpoons H^+ + HSO_3^- \tag{4.10}$$

Furthermore, HSO_3^- can form SO_3^{2-}, sulfite [22].

$$HSO_3^- + OH^- \rightleftharpoons H_2O + SO_3^{2-} \tag{4.11}$$

Whether the formation of HSO_3^- or the formation of SO_3^{2-} will dominate is shown to be highly pH dependant [22].For pH levels at 8 or above, the formation of SO_3^{2-} dominates [22]. Figure 4.1 illustrates the formation of different S(IV) depending on pH.

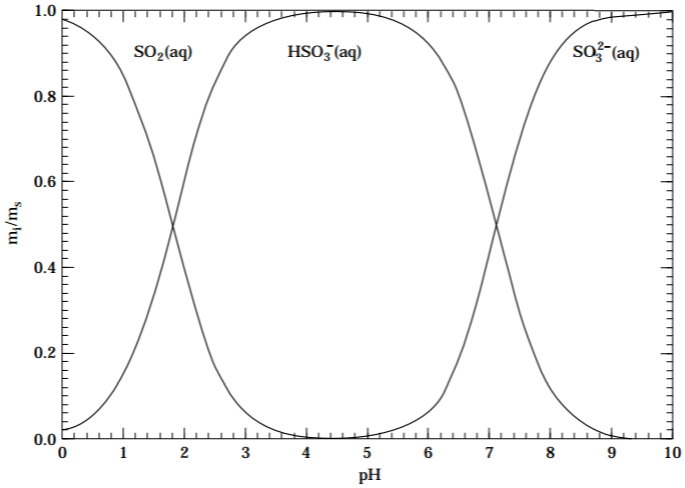


Figure 4.1: The effect of pH on S(IV). The amount of SO_2 (aq), HSO_3^-, SO_3^{2-} present is expressed in the form of mass fraction. Retrieved from Siddiqi et al. (1996) [22]

4.2.2 Absorption of NO_x

The absorption of NO_x gases into the liquid phase is more complex than the absorption of SO_2. Not only is the gas-phase NO_x in equilibrium with the liquid phase, but equilibrium and kinetic reactions also occur in the gas-phase. This complicates the absorption chemistry of NO_x, since different nitrogenous compounds are formed in the gas phase, that can also be dissolved into the liquid phase, which leads to different possible reactions that occur in the liquid phase. NO_x, in the form of NO or NO_2, can be absorbed into the liquid phase.

$$NO(g) \rightleftharpoons NO \cdot H_2O \tag{4.12}$$

$$H_{NO} = [NO \cdot H_2O]/p_{NO} \tag{4.13}$$

NO_2 has a high solubility, and is easily dissolved compared to NO, which makes it more suited in absorption processes where a high degree of absorption of NO_x is wanted.

$$NO_2(g) \rightleftharpoons NO_2 \cdot H_2O \tag{4.14}$$
$$H_{NO_2} = [NO_2 \cdot H_2O]/p_{NO_2} \tag{4.15}$$

NO_2 can, in liquid phase, react with water to form nitrous acid (HNO_2) and nitric acid (HNO_3). Furthermore, these acids deprotonate in an equilibrium reaction.

$$2NO_2 + H_2O \rightarrow HNO_2 + HNO_3 \tag{4.16}$$
$$HNO_2 \rightleftharpoons H^+ + NO_2^- \tag{4.17}$$
$$HNO_3 \rightleftharpoons H^+ + NO_3^- \tag{4.18}$$

HNO_2, as well as HNO_3, can also be formed in the gas phase and dissolve into the liquid phase. Nitrous acid has the possibility of forming NO, NO_2 in an equilibrium reaction [10]. This reaction is less likely to occur in an environment where pH$\geq$5 [23].

$$2HNO_2(aq) \rightleftharpoons NO + NO_2 + H_2O \tag{4.19}$$

Since the solubility of NO is relatively low, the component is likely to return to gas phase.

4.2.3 Nitrogen and Sulphur Interactions

Interactions in liquid phase between S(IV), HNO_2 and NO_2 are complex and difficult to map and there is an array of reactions that can occur [23]. Studies by Sima et al (2016) [23] shows that there is a possibility of reducing the number of pathways that occur withing a range of pH=1-5, hence highlighting which pathways that will dominate.

The interactions that occur between HNO_2 and HSO_3^- have been shown to be prominent in liquid phase. At pH$\geq$4, the formation of hydroxylamine disulfonic acid ($HON(SO_3)_2^{2-}$) dominates (see equation 4.20) while at pH$\leq$1 the formation of nitrous oxide (N_2O) dominates (see equation 4.21).

$$HNO_2 + 2HSO_3^- \rightarrow HADS + H_2O \tag{4.20}$$

$$HNO_2 + HSO_3^- \rightarrow 0.5N_2O + HSO_4^{2-} + 0.5H_2O \tag{4.21}$$

The formation of N_2O is undesired, since it is also a major pollutant and green house gas. Hence, it is best to keep pH levels above 4 in order to avoid the formation of unwanted N_2O.
When pH$\geq$5, dissolved nitrous oxides (NO_2) reacts with bisulfate (HSO_3^-) to form S(VI) (H_2SO_4, HSO_4^-, SO_4^{2-}) and nitrous acid (HNO_2, NO_2^-).

$$2NO_2 + HSO_3^- + H_2O \rightarrow SO_4^{2-} + 3H^+ + 2NO_2^- \tag{4.22}$$

Overall Nitrogen and Sulphur Interactions

Figure 4.2 illustrates a summary of the overall reaction pathways that occur when NO_2/SO_2 is absorbed in to the liquid phase from gas phase. The dashed lines show the pH dependant mechanisms. furthermore, the oxidation of NO to NO_2, in this case, using H_2O_2 as an oxidising agent, is illustrated.

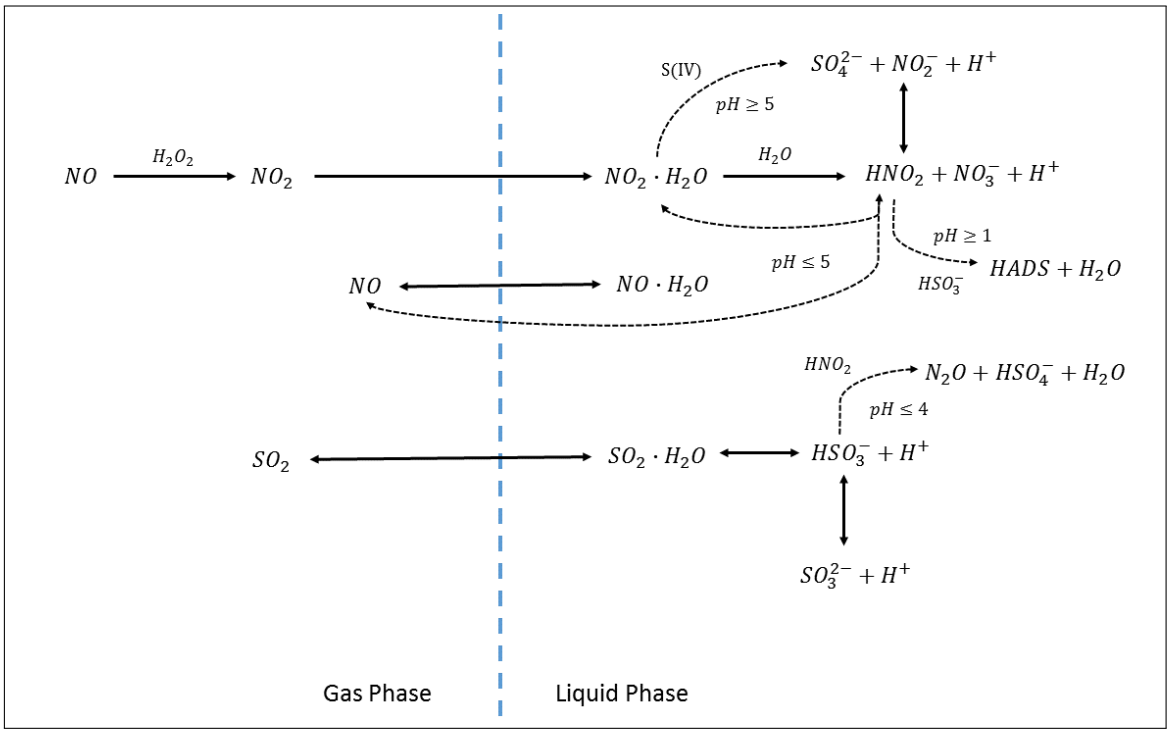


Figure 4.2: An overview of the mechanisms that occur in the liquid phase. The dashed lines are reactions that occur dependant on the pH level which are specified next to the line. HADS is a an abbreviation for hydroxylamine disulfonic acid ($HON(SO_3)_2^{2-}$). Worth noting is that the reactions mechanisms in the figure are not stoichiometrically balanced.

4.3 Mass Transfer

According to the two-film model, two meeting fluids, are separated by a boundary layer, or film, that is stagnant and with a certain thickness. For a component i, the mass transfer that occurs when the component is absorbed from one fluid into another, governed by molecular diffusion [24]. The mass transfer is dependant on there being a driving force and a contact surface where mass transfer occurs [21].

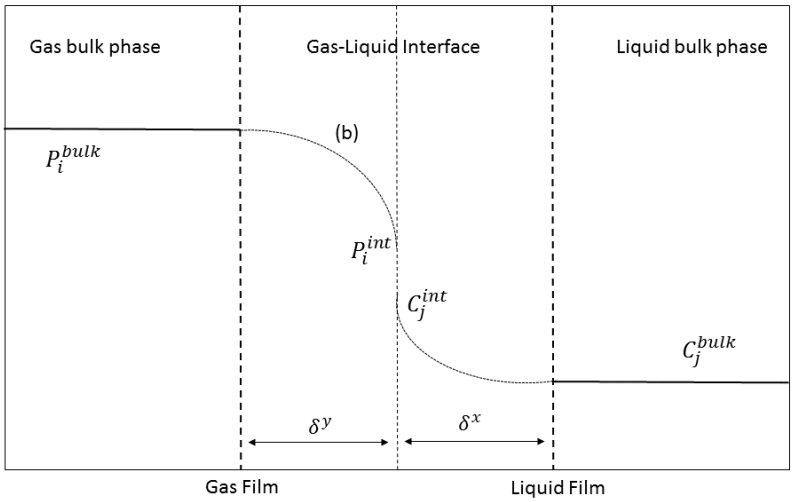


Figure 4.3: A concentration profile of the mass transfer of component i as a function of concentration in the liquid phase and partial pressure in the gas phase. δ denotes the thickness of the film

At the gas-liquid interface, equilibrium is assumed [24], and this means that the composition, in term of concentration in both gas and liquid phase, can be derived from Henry's law as:

$$C_i^L = \frac{C_i^G}{H_i} \tag{4.23}$$

Where L is used to denote the liquid phase, and G denotes the gas phase. Since only molecular diffusion is assumed to occur, Fick's law can be applied. This means that the mass flux (N_i) [mol l^{-1} s^{-1}] through the film can be expressed, for a component i, as a function of mass transfer coefficient ($k_{L,G}$), the liquid-gas interface a [m^2], and the driving force expressed in terms of concentration (C_i) [mol l^{-1}] in liquid phase and in terms of partial pressure (P_i) [bar] in the gas phase [24].

$$N_i^G = k_G a(P_i^{bulk} - P_i^{int}) \tag{4.24}$$

$$N_i^L = k_L a(C_i^{bulk} - C_i^{int}) \tag{4.25}$$

where *int*, in the equations above, denotes the film region, and *bulk* the bulk region. $k_{L,G}$ [m s^{-1}] a function of the diffusivity D [m^2 s^{-1}] and the thickness of the film δ [m]. Since it's not possible to measure the concentration of a species at the interface, an overall mass transfer coefficients ($K_{L,G}$) are used.

$$N_i^G = K_G(P_i^* - P_i^{bulk}) = K_G(H_i C_i^L - C_i^{bulk}) \tag{4.26}$$

$$N_i^L = K_L(C_i^{bulk} - C_i^*) = K_L(C_i^{bulk} - \frac{C_i^G}{H_i}) \tag{4.27}$$

The resistance in the gas and liquid film can be expressed though $K_{G,L}$

$$\frac{1}{K_G} = \frac{H_i}{k_l} + \frac{1}{k_G} \tag{4.28}$$

$$\frac{1}{K_L} = \frac{H_i}{k_l} + \frac{1}{k_G H_i} \tag{4.29}$$

which is a sum of resistances through the gas and liquid film.

5
Method

This work is based on a case study of the Green Tech Marine Scrubber by Yara Marine Technology, and installed into a cruise ship. The method approach for this work is to firstly construct a flowsheet of the open loop and closed loop SO_2 scrubber in Aspen Plus. This model is then validated, this by using operational data provided by Yara Marine Technology and comparing the operational data, in terms of SO_2 removal efficiency, with the generated simulation results. If simulation results correspond the operational data, the Aspen Plus model is accepted and used for modelling the NO_x and SO_2 scrubber process in RateSep.

5.1 Case Study

5.1.1 Exhaust Gas and Seawater Composition

The SO_2 composition is retrieved from the log data, and it is assumed that a fuel oil containing 3.5% sulphur produces 900 ppmv SO_2 when the exhaust gas leaves the engine. The amount of NO_x in the exhaust gas is dependent on the type of engine, this data is provided by Yara Marine Technology. It is assumed that 10% of the NO_x formed in the combustion engine is converted to NO_2, while 90% is NO. Other typical exhaust gas compositions are retrieved from MAN, 2004 [25] for heavy fuel oil.

Table 5.1: The exhaust gas properties of the ingoing gas stream. The exhaust gas is only comprised of gaseous components and particulate matter is disregarded.

Exhaust gas inlet temperature:	360 C
Exhaust gas inlet pressure:	1.0103 bar
Exhaust gas composition (mass basis):	
	N_2: 75.8%
	O_2: 12.97%
	H_2O: 5.94%
	CO_2: 5.1%
	SO_2 (3.5-3.36% S): 900 ppmv (3.5%)
	NO_2: 73 ppmv
	NO: 658 ppmv

Particulate matters in the exhaust gas is disregarded, and it is assumed that all fuel has been consumed in the marine diesel engine. Furthermore, it is assumed that all

NO_x oxidised and converted to NO_2 when entering the absorber using an oxidising agent. Regarding the removal of SO_2, the objective is to remove about 98%. This should correspond to a fuel sulphur concentration of 0.1%, which fulfils the emission regulations within the ECA.

Table 5.2: Basis for liquid stream properties. Values are based on information given by Yara Marine Technology and literature values [2].

Temperature:	20 °C
Pressure:	2.0 bar
Average droplet diameter at nozzle:	D_V=1200μm
Seawater composition at salinity 35 ppt [2]:	
	$HCO3^-$: 0.108 g/kg_{H_2O}
	CO_3^{2-}: 0.016 g/kg_{H_2O}
Closed-loop:	
MgO composition: 25% $Mg(OH)_2$, 75% H_2O	

According to Andreasen (2007) [2], the alkali contribution in sea water, is mainly due to absorbed CO_2 from the atmosphere into liquid phase. Furthermore, Andreasen [2] estimates that the composition of $HCO_3^- = 2400\mu mole/kg_{H_2O}$ can be set to approximate the alkalinity of the seawater. In Aspen Plus, this generates that $pH = 8.1$ in the liquid stream.

5.2 Process Simulation

5.2.1 Flowsheeting

The process modelling was performed in Aspen Plus V8.8. Aspen Plus is a steady-state simulator, commonly used for process design and optimisation for commercial and academic purposes. The absorption process is simulated using RateSep, which is often used in rigorous separation-type modelling involving kinetics and when electrolytes are present. The process simulation of the SO_2 scrubbing is divided into two separate simulations; one open-loop simulation and one closed-loop simulation.

The open loop scrubber has a stream splitter that evenly distributes the liquid across the scrubber into four streams of equal size. For closed-loop modelling, a purge stream and a makeup stream is added to the recycle, in order for mass balance calculations to converge. This since Aspen Plus simulates in steady-state, where no accumulation is assumed. This is done by setting a balance block calculator over the ingoing and outgoing streams (gas inlet and outlet, makeup and purge stream), which allows the system to be operated in steady-state.

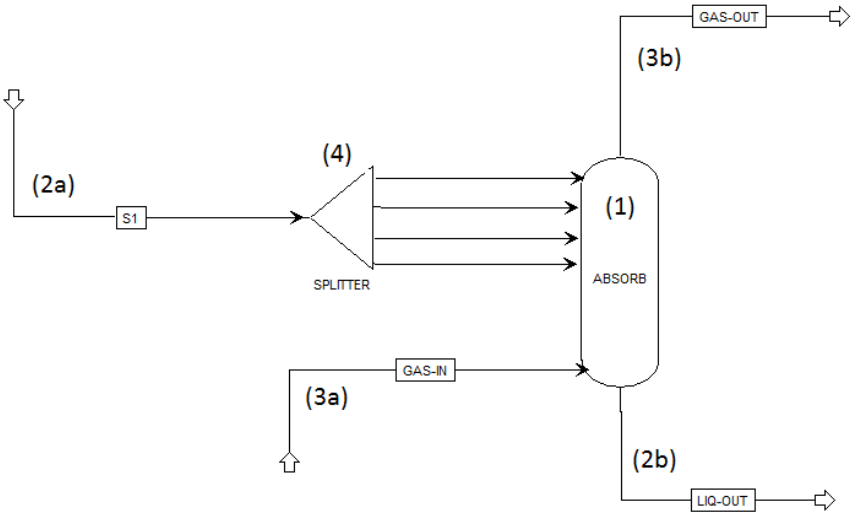


Figure 5.1: The simulation set-up of the Aspen Plus absorber model in open-loop. The model constitutes of (1) absorber tower (2a) Inlet liquid stream of seawater (2b) Outlet stream of seawater (3a) Inlet exhaust gas stream (3b) Outlet exhaust gas stream. (4) Stream splitter that splits the liquid feed into four even streams that is distributed evenly across the scrubber.

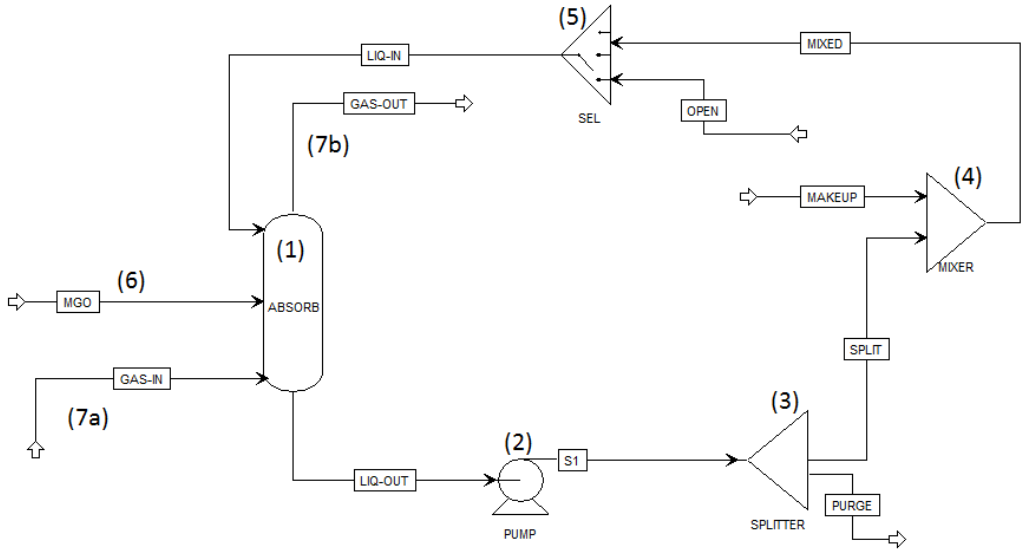


Figure 5.2: The simulation set-up of the closed-loop Aspen Plus model. A recycled stream makes up the wash water. The simulation is composed of (1) Absorber tower (2) pump (3) Splitter with a purge stream (4) Mixer with a makeup stream (5) Selector (6) $Mg(OH)_2$ addition stream (7a) Exhaust gas inlet (7b) Exhaust gas outlet

ELECNRTL is used to predict the thermodynamic properties, which is an extension of the NRTL (Non-Random Two-Liquid) model that includes electrolytes. ELECNRTL is best suited for a multi-solvent system where electrolytes are present in an

aqueous environment.

5.2.2 Validation Method

An open loop model is constructed in Aspen Plus, using RateSep. The approach for the validation is to pick case points from the log data that is representative of the open loop system. Each case point consists of three main parameters that are specific for each case: liquid flow rate [kg/s], exhaust gas flow rate [kg/s], and SO_2 composition [ppmv] in the exhaust gas. The model is validated against one output parameter, that is also specified in the log data, which is the outgoing SO_2 exhaust gas composition [ppmv]. The RateSep model is adjusted and to the case points, so that the input parameters, produce similar output parameter as specified in the log data. In order to validate that the model is representative of the case, other input parameters from the log data are tested without adjusting or fitting the model. If the RateSep model is able to produce similar results to the log data, the model is validated. This model is then used for simulating nitrogen and sulphur chemistry in the open loop and closed loop flowsheets.

5.2.3 RateSep Modelling

Since there is no direct method for simulating an absorption spray tower i Aspen Plus V8.8, a packed absorption column is used in RateSep. The RateSep model is then adjusted to resemble a spray-type absorber by making assumptions.
Firstly, the specific packing area (a_p) in RateSep is calculated by assuming the following:

- All droplets can be considered spherical.
- The void fraction is assumed to be $\varepsilon = 0.98\ m^2/m^3$.

When assuming a void fraction, i.e. the space where there is no gas-to-liquid contact, an expression for the specific surface area a_p $[m^2/m^3]$ can be derived, as seen in equation 5.1.

$$a_p = \frac{6(1-\varepsilon)}{D_V} \tag{5.1}$$

The assumption is that a random packing contact surface corresponds to the liquid-gas contact surface between the exhaust gas and the water droplets in the spray absorber, for a specific void fraction (ε) and droplet diameter (D_V) [m]. The derivation of the expression for a_p can be found in appendix A. The configuration of the RateSep absorber can be seen below, in table 5.3.
The effectiveness of the absorber corresponds to the amount of SO_2 and NO_2 absorbed by the unit. The components are expressed in terms of mole fractions in the exhaust gas.

$$X_{SO_2,NO_2} = \frac{\dot{n}_{SO_2,NO_2}}{\dot{n}_{Total}} \tag{5.2}$$

Where $\dot{n}$ is the molar flow (mole/s) of exhaust gas. The effectiveness can be defined as percentage of removed components from the exhaust gas:

Table 5.3: The base model in the Aspen Plus V8.8 using RateSep

Packing Height:	9.6 m
Diameter:	2.3 m
Packing type:	Pall Rings (90mm)
Working pressure:	2 bar
Contact surface (a):	100 m^2/m^3
Void Fraction (ε):	0.98 m^3/m^3

SO_2 removal:

$$Removal(\%) = \frac{X_{in,SO_2} - X_{out,SO_2}}{X_{in,SO_2}} \cdot 100\% \tag{5.3}$$

NO_2 removal:

$$Removal(\%) = \frac{X_{in,NO_2} - (X_{out,NO_2} + X_{out,NO})}{X_{in,NO_2}} \cdot 100\% \tag{5.4}$$

In order to comply with sulphur regulations set by MARPOL, a SO_2 removal efficiency of 98% can be assumed to correspond to the most stringent regulation that exists within the ECA (0.5% sulphur content). For NO_2, it is desirable to achieve as high conversion as possible to comply with Tier III regulation.

5.2.3.1 Rate-Based Modelling

By utilising rate-based model (RateSep), instead of an equilibrium-based, factors such as mass transfer resistances, liquid hold-ups, interfacial area, and two-film modelling, are included in the simulation. The following section reviews these factors and the adjustments that have been made to the rate-based model.

Flow Model
There are several flow models that can be used in RateSep; one of those is the mixed flow model. The mixed flow model determines bulk properties and calculates the rate of reaction as well as the mass fluxes over the liquid and gas film, this by assuming that all parameters are independent of the position and mixing is perfect. This model is also the default flow model in RateSep. The liquid film is discretised using Discrxn in RateSep into the following partitions: 10^{-6}, 10^{-5}, 10^{-4}, 10^{-3}, 0.01, 0.1, 0.5. This approach can be helpful when there are fast reactions involved.

Mass Transfer Coefficient and Interfacial Area
The mass transfer is calculated using the Onda (1986) [26] correlation for mass transfer coefficient and the interfacial area. In RateSep, the correlations for the mass transfer coeffiencents for packed absorbers are highly empirical, and depend

on the Schmidt number, the type of packing, as well as the gas-side and liquid-side flow rates.

$$k_V = f(Re_V, Sc_V, a_p) \qquad [m/s] \tag{5.5}$$

$$k_L = f(Re_L, Sc_L, a_p) \qquad [m/s] \tag{5.6}$$

For this model, the liquid side mass transfer coefficient (k_L) is decreased by a factor of 100 since it is assumed that the liquid side mass transfer for a spray type scrubber has a lower value than for a packed.

$$0.01 k_L(Packed\ Bed) = k_L(Spray) \tag{5.7}$$

The interfacial area is derived from the specific surface area (a_p).

$$a^I = a_w A_t h_p \qquad [m^2] \tag{5.8}$$

$$a_w = f(a_p, Re_L, Fr_L) \qquad [m^2/m^3] \tag{5.9}$$

a_w is the wetted area, and directly proportional to the specific surface area.
Furthermore, the spray absorber is assumed to have lower mass transfer rates as a result of reduction in interfacial area (a_i) [27]. The void fraction (ε) is used to calculate the volumetric liquid hold-up (h_L), using a built-in Stichlmair correlation in Aspen RateSep.

$$h_L = h_t h_p A_t \qquad [m^3] \tag{5.10}$$

h_t is the fractional liquid hold-up and a function of the void fraction (ε), h_p [m] is the packing height, A_t [m^2] the cross-sectional area. Furthermore, it is assumed that mass transfer occurs along the entire length of the absorption tower modelled in Aspen Plus V8.8, which corresponds to 60% of the actual length of the tower.

5.3 Liquid-phase Chemistry

In the absorber, all reactions are assumed to occur in the liquid phase. Hence, gas phase reactions are not reviewed and assumed to not occur within the absorber. There are two main types of reactions occurring: rate-controlled reactions and equilibrium reactions. All formations of salts or solids, mainly generated by the addition of $Mg(OH)_2$, are neglected.

5.3.1 Rate-controlled reactions

To calculate the reaction rate for a rate-controlled reaction, Aspen uses a built-in reduced power law.

$$r = kT^n e^{\frac{-E}{RT}} \Pi C_i^{\alpha_i} \tag{5.11}$$

E: [J/mole]
k: $[s^{-1}]$
r: [L, mole, s]
C_i: [mole/L]
T: Celsius

For this work, the rate-controlled reactions, in liquid phase, that have been used are specified in table 5.4. Only liquid-phase reactions are assumed to occur in the Absorber. The rate-based reactions include reactions involving nitrogen dioxide and the nitrogen and sulphur (N-S) interactions.

5.3.2 Equilibrium reactions

Aspen Plus uses a built-in expression to calculate the equilibrium constant, equation 5.12. In table 5.5 the equilibrium reactions used in the simulation is listed.

$$ln(K_{eq}) = A + \frac{B}{T} + C \cdot ln(T) + D \cdot T \tag{5.12}$$

K_{eq}: L·mole
T: Celsius [°C]
A, B, C, D: constants

The equilibrium reactions involve nitrogen and sulphur reactions, as well as dissolved carbon dioxide and the dissociation of $Mg(OH)_2$, which can be seen in table 5.5.

Table 5.4: Rate-controlled reaction formulas and the rate expression

	Reaction Formula	
	Nitrogen reactions:	
R_1	$2\,NO_2 + 2\,H_2O \rightarrow HNO_2 + HNO_3$	
R_2*	$2\,HNO_2 \rightarrow NO + NO_2 + H_2O$	
R_3*	$NO + NO_2 + H_2O \rightarrow 2\,HNO_2$	
	N-S reactions:	
	$1 <$ pH < 4	
R_4	$HNO_2 + 2\,HSO_3^- \rightarrow HADS + H_2O$	
R_5	$HNO_2 + HSO_3^- \rightarrow 0.5\,N_2O + HSO_4^{2-} + 0.5\,H_2O$	
	pH ≥ 4	
R_4	$HNO_2 + 2\,HSO_3^- \rightarrow HADS + H_2O$	
	pH ≤ 1	
R_5	$HNO_2 + HSO_3^- \rightarrow 0.5\,N_2O + HSO_4^{2-} + 0.5\,H_2O$	
	pH ≥ 8	
R_6	$2\,NO_2 + SO_3^{2-} + H_2O \rightarrow SO_4^{2-} + 2\,H^+ + 2\,NO_2^-$	
	pH ≥ 5	
R_7	$2\,NO_2 + HSO_3^- + H_2O \rightarrow SO_4^{2-} + 3\,H^+ + 2\,NO_2^-$	
	Rate Expression $[L, mole, s]$	Reference
	$r_{R_1} = 1 \cdot 10^8 C_{NO_2}^2$	[28]
	$r_{R_2} = 13.4 C_{HNO_2}^2$	[30]
	$r_{R_3} = 1.6 \cdot 10^8 C_{NO_2} C_{NO}$	[30]
	$r_{R_4}:\ k = 1.887 \cdot 10^9,\ E = 5.075 \cdot 10^7\ J/kmol$	[23]
	$r_{R_5}:\ k = 1.11 \cdot 10^9,\ E = 5.075 \cdot 10^7\ J/kmol$	[23]
	$r_{R_6} = r_{R_6} + r_{R_7} = k_{pH} C_{NO_2} (C_{HSO_3^-} + C_{SO_3^{2-}})$	[31]
	$k_{pH=5.3} = 1.24 \cdot 10^7\ [s^{-1}]$	
	$k_{pH=6.7} = 1.54 \cdot 10^7$	
	$k_{pH=6.8} = 1.34 \cdot 10^7$	
	$r_{R_7} = r_{R_6} + r_{R_7} = 0$	[31]

*Note that reactions R_2 and R_3 do not occur in an environment where pH exceeds 5 [23].

Table 5.5: Equilibrium reaction formulas and the equilibrium constants

	Reaction Formula	
	Sulphur reactions:	
R_8	$SO_2\,(g) \rightleftharpoons SO_2\,(aq)$	
R_9	$SO_2\,(aq) + H_2O \rightleftharpoons HSO_3^- + H^+$	
R_{10}	$HSO_3^- \rightleftharpoons H^+ + SO_3^{2-}$	
	Nitrogen reactions:	
R_{11}	$HNO_2 \rightleftharpoons H^+ + NO_2^-$	
R_{12}	$HNO_3 \rightleftharpoons H^+ + NO_3^-$	
	Other:	
R_{13}	$CO_2 + H_2O \rightleftharpoons HCO_3^- + H^+$	
R_{14}	$HCO_3^- \rightleftharpoons CO_3^{2-} + H^+$	
R_{15}	$H_2O \rightleftharpoons OH^- + H^+$	
R_{16}	$Mg(OH)_2(aq) \rightleftharpoons MgOH^+OH^-$	
R_{17}	$MgOH^+OH^- \rightleftharpoons Mg^{2+} + 2OH^-$	
	Equilibrium constants $[L \cdot mole]$	Reference
	$K_{eq,R_9} = 5.1 \cdot 10^{-4}$	[22]
	$K_{eq,R_{10}} = 15.4$	[22]
	$K_{eq,R_{11}} = 1.39 \cdot 10^{-2}$	[30]
	$K_{eq,R_{12}} = 6.24 \cdot 10^{-8}$	[28]
R_{13}	$A = 231.465, B = -12092.1, C = -36.7816$	[32]
R_{14}	$A = 216.049, B = -12431.7, C = -35.4819$	[32]
R_{15}	$A = 132.899, B = -13445.9, C = -22.4773$	[32]

6
Validation

The model is validated by using the RateSep open loop configuration by choosing a set of data from the case study operational data and fitting the RateSep open loop model to the data set. The data set that is used can be seen in Table 6.1.

Table 6.1: Data set of the case study Green Tech Marine Scrubber in open loop configuration. When simulating in RateSep, the SO_2 outlet is the result while the rest are input values.

	Liquid Feed [kg/s]	**Exhaust Gas Feed** [kg/s]	**L:G ratio** -	**SO_2** ppmv (inlet:outlet)
1	189.4	18.5	10.23	843:21
2	180	18.6	9.67	843:23
3	170	18.6	9.14	864:30
4	160	18.6	8.6	864:42
5	150	18.6	8.0	864:53
6	140	18.4	7.6	864:61

In RateSep, there is a possibility of tuning the simulation model to fit the operational data, this by multiplying the liquid interfacial area (a^I) by a factor from anywhere between 10^{-8} to 10^8. In order for the simulation results to coincide with the data set in Table **??** each data points is tuned until it the data set and the simulation shows the same results.

6.1 Results

Figure 6.1 shows that for each point, there is an increase in the interfacial area. By assuming that there is a relationship between the liquid feed and the interfacial area, a regression can be made which gives the linear function shown in Equation 6.1.

$$y = 0.0032x + 0.64 \tag{6.1}$$

Where y is the fractional increase in interfacial area (%) and x is the liquid feed rate [kg/s]. In order to asses if this correlation is valid and can be used, further simulations are made with the help of a new operational data set in open loop operations. The results of these simulations can be seen in Figure 6.2.

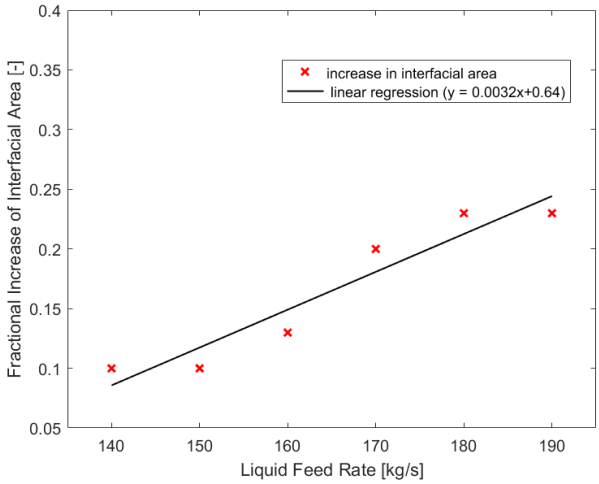


Figure 6.1: For each data point, a^I is increased by a factor of 0.1-0.25 in order for the simulation results to coincide with the SO_2 outlet in data set.

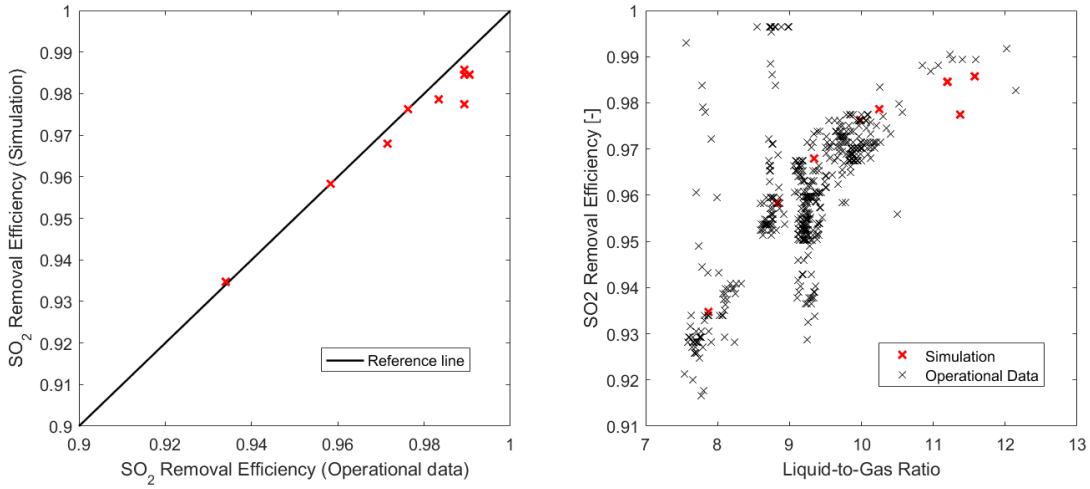


Figure 6.2: A comparison between the simulation and a new data set shows that the liquid interface correlation works overall for simulating the case study scrubber.

Figure 6.2 shows the results of simulating new operational data point for the scrubber in open loop mode. The first part shows a comparison between the removal efficiency from the operational data and the resulting removal efficiency of the simulation. The second plots the same results but in the context of liquid-to-gas ratio and removal efficiency, along with all of the operational data points. The conclusion that can be made is that the simulation follows the same trend as the overall open loop operational data points. Overall, Figure 2 shows that the simulations, using the linear correlation for the interfacial area, are within a good range of the performance of the scrubber for open loop operational mode. The data set for used in Figure 6.2 can be seen in Appendix A.

The correlation in Equation 6.1 is further used in the closed loop operational mode. The following data (Table 6.2) set is used to validate the RateSep model in closed loop mode:

Table 6.2: Data set of the case study Green Tech Marine Scrubber in closed loop configuration.

	Liquid Feed [kg/s]	**Exhaust Gas Feed** [kg/s]	**MgO Dosing** [litre/min]	**SO_2** ppmv (inlet:outlet)
1	140	18.6	7.6	843:21
2	140	18.7	6.7	864:17
3	140	18.7	6.2	864:15

Figure 6.3 shows that the closed loop simulation is within the same range as the data set for the closed loop operational mode.

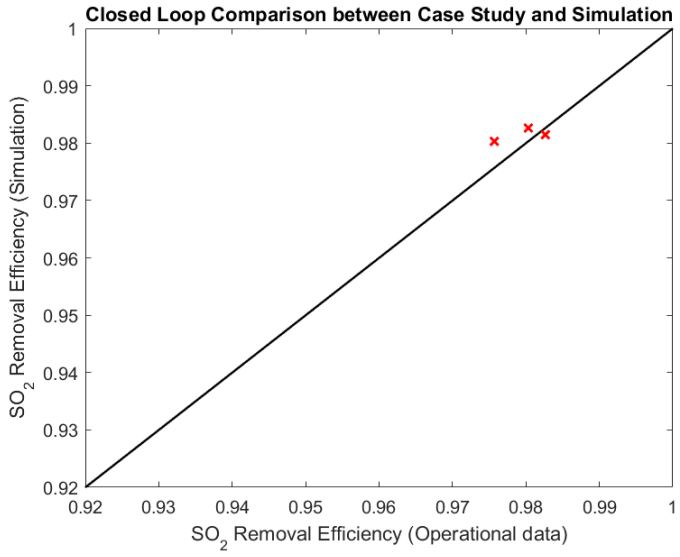


Figure 6.3: A comparison between the simulation and a new data set shows that the liquid interface correlation works overall for simulating the case study scrubber.

7

Evaluation of the Combined NO_x/SO_2 system

Following chapter presents the result from the RateSep simulation, for the open and the closed operational mode when modelling the nitrogen and sulphur chemistry. The optimisation of the scrubber includes: the liquid flow rate optimisation, residence time optimisation (height), and the choice of oxidising agent.

7.1 Evaluation of Open Loop Operational Mode

7.1.1 Evaluation of liquid flow rate and removal efficiency

The RateSep simulation for scrubbing both SO_2 and NO_2 shows an improvement in efficiency regarding the increased absorption of SO_2 as well as a high absorption rate of NO_2.

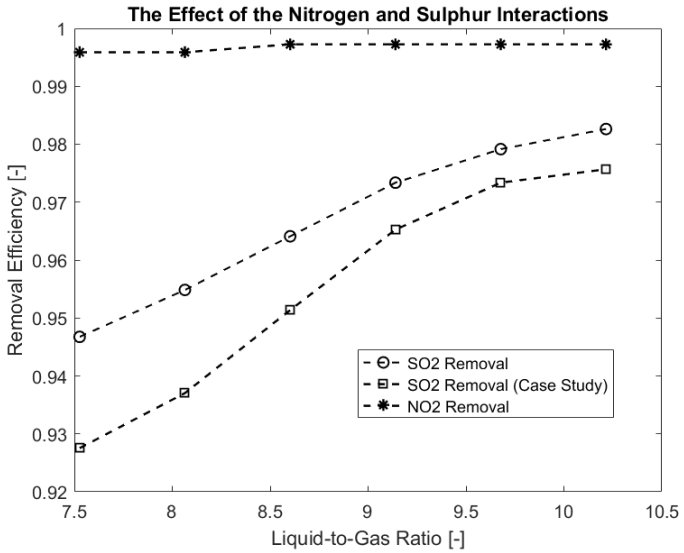


Figure 7.1: The removal of SO_2 as a result of the interactions between NO_2 and SO_2 in liquid phase. For all liquid flow rates, gas rates remain constant (18.6 kg/s) as well as the ingoing gas composition (x_{SO_2}=864 ppmv, x_{NO_2}=731 ppmv).

Figure 7.1 shows that the nitrogen and sulphur interactions has an effect on the absorption of SO_2. The effect is greater at low liquid flow rates (140-160 kg/s). The

absorption of NO_2 was constant for every liquid flow rate (99%), however, N_2O was found in the outgoing exhaust gas (25-18 ppmv), which is a result of pH<4 in the scrubber. In order to avoid the formation of N_2O, the pH needs to be increased. Since MgO i available in closed loop mode, this could also be used in the open loop mode. This could overall further benefit the absorption of SO_2.

7.1.1.1 Reaction profiles

The nitrogen and sulphur reactions that occur in the scrubber is highly dependent on the pH levels. In order to control the pH levels in the scrubber, seawater is used. The seawater is distributed over the scrubber through four inlets, this in order to ensure that the pH level doesn't decrease to low levels (pH≤4) in the early stages. Figure 7.2 shows the pH levels produced for a liquid flow rate of 190 kg/s for each theoretical stage, as well as the formation of chemical components as a result of the nitrogen and sulphur chemistry.

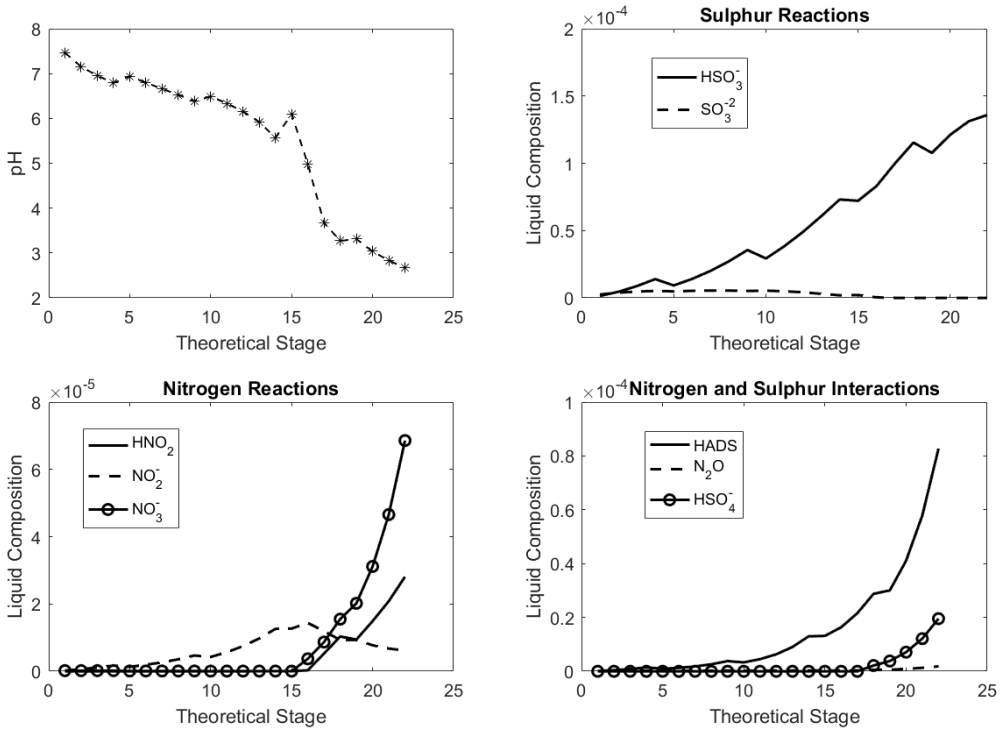


Figure 7.2: The pH and liquid phase composition in the open loop scrubber for a liquid flow rate 170 k/s, exhaust gas rate 18.6 kg/s, x_{SO_2}=864 ppmv, x_{NO_2}=731 ppmv

Even if there is an increase in removal efficiency, as seen in Figure 7.1, the pH profile in the RateSep model shows that there is a need for pH control in order to keep pH levels above 4. This could result in a greater removal efficiency with regards to SO_2. The composition plots in 7.2 shows that there is plenty of HSO_3^- in the system compared to SO_3^{2-}, this is desirable in this case, since it promotes the formation on HADS. Also, due relatively high pH levels (pH=8-5), HNO_2 is likely to dissociate in to NO_2^-, which the figure also shows.

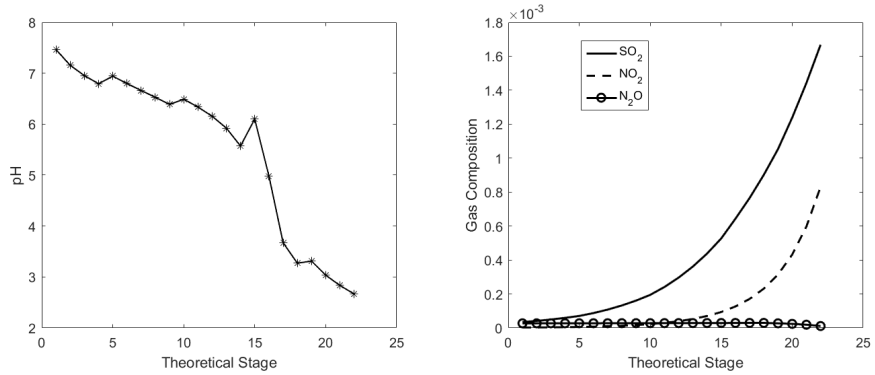


Figure 7.3: The pH and gas phase composition in the open loop scrubber for a liquid flow rate 170 k/s, exhaust gas rate 18.6 kg/s, x_{SO_2}=864 ppmv, x_{NO_2}=731 ppmv

7.1.2 Evaluation of scrubber height and removal efficiency

In order to asses the affect the residence time has on the scrubber efficiency, a sensitivity analysis (figure 7.4) is performed on the open loop scrubber system by altering the height of the scrubber. This is done for three different liquid flow rates (170, 180, 190 kg/s), other parameters, such as exhaust gas composition and exhaust gas flow rates, have been kept constant.

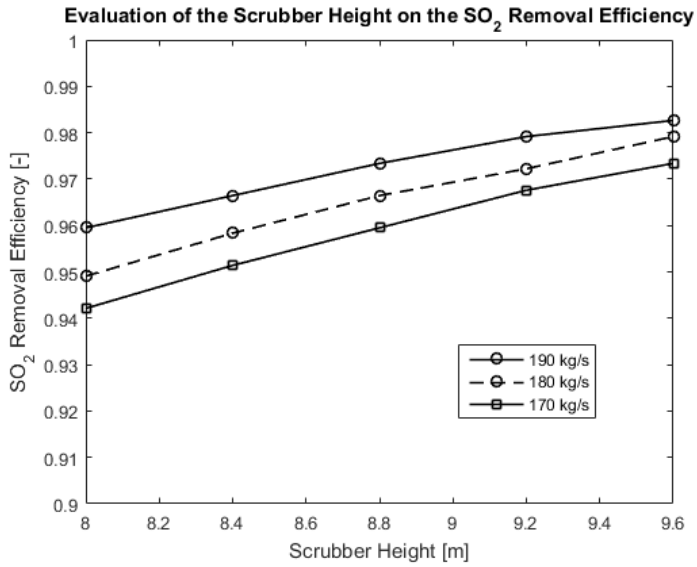


Figure 7.4: The sensitivity analysis shows that height has a great impact on the conversion of SO_2 in gas phase. Exhaust gas flow rate is 18.6 kg/s, x_{SO_2}=864 ppm, x_{NO_2}=731 ppm

There are potentials in reducing the height of the mass transfer region in the scrubber as well as reducing the amount of needed seawater. Worth noting about Figure 7.4 is that even though the height is reduced by abot 60% (9.6-8), the removal of SO_2 is still within the range of 90%.

7.2 Evaluation of the Closed Loop Operational Mode

7.2.1 Evaluation of liquid flow rate and removal efficiency

Figure 7.5 shows the effect of the the NO_2 and SO_2 absorption and liquid phase chemistry, compared to only scrubbing SO_2 for recycled liquid flow rates between 135-145 kg/s.

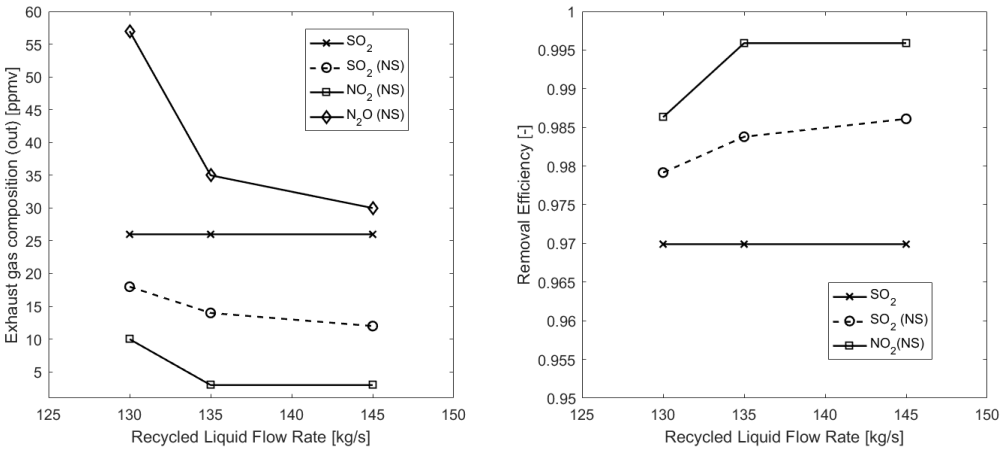


Figure 7.5: The results show the increased removal of SO_2 when the nitrogen and sulphur chemistry is involved. The amount of liquid recycled is varied between 130-145 kg/s and the amount of MgO is set to 6 litres/min for all cases. x_{SO_2}=864 ppm, x_{NO_2}=731.

The NO_2 and SO_2 interactions have a great effect on the absorption efficiency of SO_2, however, the at 135 kg/s there is a noticeable formation of N_2O that is reduced by increasing the amount of liquid that is recirculated. The formation of N_2O might be due to the fact that, at 130 kg/s, it is more difficult to keep a high enough pH (pH$\geq$4) throughout the scrubber. In order to try to reduce the amount of N_2O, an attempt is made to increase the overall pH in the scrubbers, this at a liquid flow rate at 135 kg/s. By splitting the ingoing recycle stream into two streams entering at two different points, pH levels below 4 can be avoided.

The results from this attempt shows that even though the split recycle stream does not increase the removal of SO_2 or the removal of NO_2, the formation of N_2O is non-existent. It shows that if the pH is kept above 4 in the scrubber, formation of N_2O can be avoided. The pH levels throughout the scrubber when splitting the stream can be seen in figure 7.7 as well as the liquid composition of nitrogen and sulphur compounds throughout the scrubber.

7.2.2 Reaction Profiles

Figure 7.6 display the liquid compositions of nine components and the pH values in the scrubber for a liquid flow rate of 135 kg/s.

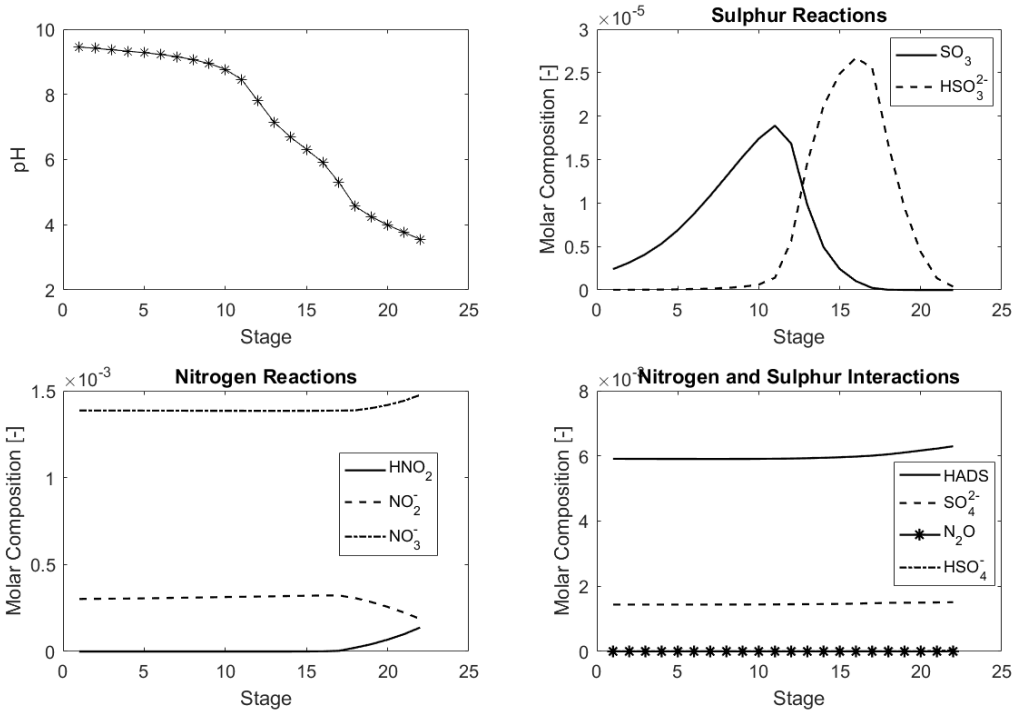


Figure 7.6: The liquid phase composition in the RateSep model as a function of the theoretical stages in closed loop.

Compared to when the system is running in open loop mode, the amount of HADS formed in the scrubber is greater. Also, the figure clearly shows that at a high pH level, the formation of SO_3^{2-} dominates, but as the pH decreases the formation of HSO_3^- increases. Compared to open loop mode, the pH is higher throughout the scrubber due to the added alkali (MgO), but drops below 4 at the very last stages.

Figure 7.7 shows the pH levels and the liquid-phase composition when a recycle stream is split.

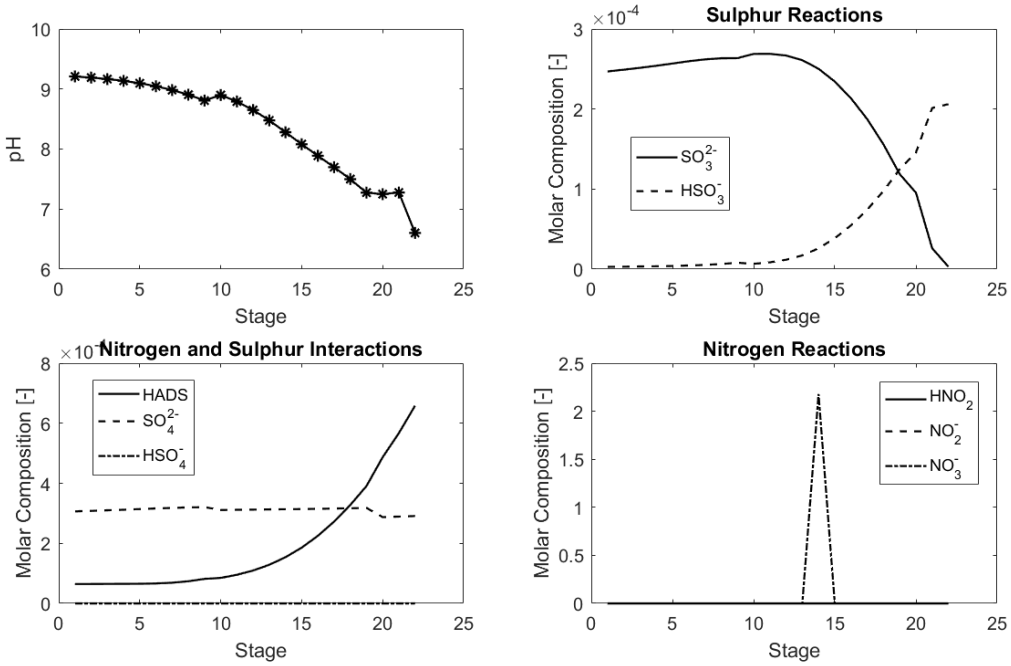


Figure 7.7: The pH and the liquid composition in the scrubber when the recycle stream is split in order to increase the overall pH throughout the scrubber. The liquid flow rate is set to 135 kg/s, and the amount of MgO is set to 6 litres/min for all cases. x_{SO_2}=864 ppm, x_{NO_2}=731.

7.2.3 Evaluation of scrubber height

The previous chapter, that reviewed the results for the open loop system, showed that there is a potential in reducing the RateSep packed height. Figure 7.8 shows the effect of reducing the packed height by 1 m, from 9.6 m to 8.6 m, on the liquid phase composition, for a closed loop system.
As figure 7.8 shows, the packing height has little effect on the formation on HADS in the liquid phase. However, there is now in more HSO_3^- and SO_3^{2-}, in terms of liquid composition, in the scrubber. This can be a results of higher pH levels since the scrubber now is reduced in packing height. Table 7.1 shows the removal efficiencies generated from reducing the packing height.

Table 7.1: The results show the removal of SO_2 and NO_2 from the exhaust gas as well as the formation N_2O as a results of reducing the packing height of the scrubber compared to the previous height of 9.6m.

Height	SO_2	NO_2	N_2O
m	ppmv	ppmv	ppmv
9.6	14 (98% Conversion)	3	35
8.6	26 (97% Conversion)	5	43

Table 7.1 shows the overall absorption efficiency with regards to SO_2 and NO_2.

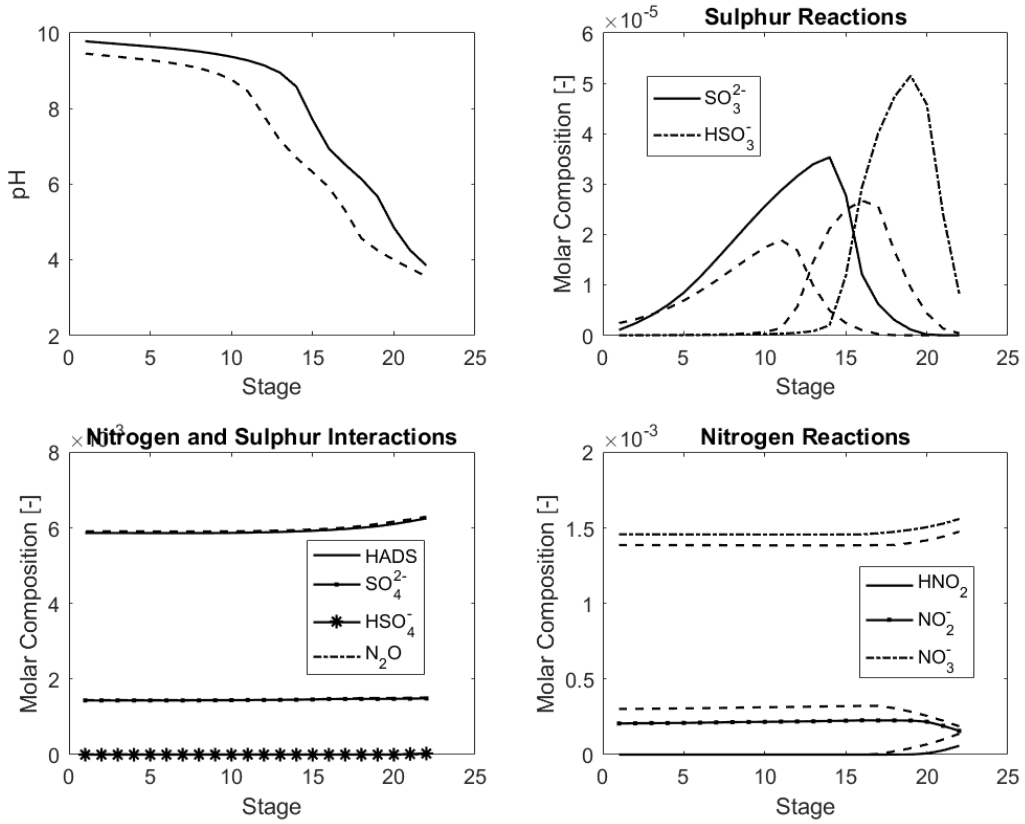


Figure 7.8: The liquid phase compositions in the scrubber for a liquid flow rate of 135 kg/s, where the dashed lines denote the case study model where the packing height is 9.6 m and the filled line denotes the composition for the model where the height is reduced to 8.6 m. Exhaust gas compositions are x_{SO_2}= 864 ppm and x_{NO_2}=731 ppm and flow rates are: 135 kg/s, 18.6 kg/s and 6 litres/min

Reducing the packing height, without changing the recycled liquid flow, has an effect on the SO_2 conversion efficiency.

7.3 Choice of oxidant: converting NO to NO_2

This section evaluates hydrogen peroxide (H_2O_2) and chlorine dioxide (ClO_2) as oxidising agents. All other side reactions involving NO and the oxidising agent, that might interfere with the oxidation of NO to NO_2, are not regarded.

7.3.1 H_2O_2 as an oxidising agent

The amount of hydrogen peroxide needed is derived with the help of reaction stoichiometrics, along with a 20% stoichiometric excess. Table 7.2 shows the results (see Appendix A for detailed calculations).

Table 7.2: The amount of H_2O_2 needed to oxidise NO for a maximum gas flow rate

Conversion rate:	**0%**	**100%**
NO [ppmv]	658	0
NO_2 [ppmv]	73	731
H_2O_2:NO	-	1.8
Exhaust gas [kg/s]	20	20
NO [kg/hr]	88.2	88.2
NO [kmol/hr]	2.94	2.94
H_2O_2 [kmol/hr]	-	5.3
H_2O_2 [kg/s]	-	0.05

7.3.2 ClO_2 as an oxidising agent

The stoichiometric ratio (ClO_2:NO) is 0.5 and furthermore, a 20% stoichiometric excess is added. The results can be seen in Table 7.3 and for detailed calculations, see Appendix A.

Table 7.3: The amount of ClO_2 needed to oxidise NO for a maximum gas flow rate.

Conversion rate:	**0%**	**100%**
NO [ppmv]	658	0
NO_2 [ppmv]	73	731
ClO_2:NO	-	0.6
Exhaust gas (max) [kg/s]	20	20
NO [kg/hr] (max)	88.2	88.2
NO [kmol/hr]	2.94	2.94
ClO_2 [kmol/hr]	-	1.3
ClO_2 [kg/s]	-	0.033

7.3.3 Integration of oxidant into the system

The oxidation process, for both H_2O_2 and ClO_2, is rapid and utilising a reactor to oxidise NO to NO_2 can be redundant. Therefore the oxidant could be integrated into the system by constructing an injection point, preferably after the exhaust gas is leaving the diesel engine, where the oxidant comes in contact with the exhaust gas. Equipment wise, this would require that a suitable tank is constructed that is connected to the exhaust pipe with an injection point.

8
Conclusion

This work is a case study of the implementation of simultaneous NO_x and SOx absorption from a cruise ship. The work has involved the construction of a process model of the absorption system.

Validation of SO_2 absorption model
The process model was validated against operational data from a SO_2 absorption system. The mass transfer coefficient and a correlation for the dependence of the gas-liquid contact area of the liquid flow rate was fitted against a set of operational data for open-loop operation. The fitted model was then validated against a different set of data for open-loop operation as well as closed-loop operations. The model performed satisfactory. Future work should focus on validation of simultaneous NO_2 and SO_2 absorption and developing a model for a spray column.

Performance of NO_2-SO_2 absorption process
The results show that the process removes NO_x efficiently from the flue gas stream. There is also an overall improvement of the SO_2 removal compared to today's process. In open loop configuration, the formation nitrogen and sulphur is mainly bound as HADS. pH control in open loop can further increase the absorption efficiency, since the chemistry is highly pH dependent. In the closed loop configuration, due to the recirculation, there is a risk of N2O formation that must be considered. The oxidation of the NO present in the flue gas require an oxidising agent. The process would requires around 0.033 kg ClO_2/s or 0.05 kg H_2O_2/s in order to oxidise all NO. The oxidation process can occur within the exhaust gas pipeline, since the reaction mechanisms are fast. In order to asses which type of oxidant should be utilised, the determining factor is the economic feasibility and the cost of utilising and storing an oxidising agent. The handling of chemicals on-board ships is regulated by maritime law and require strict safety practises that involve the construction of chemical storage tank as well as storage size and placement. Overall, this method of absorbing both NO_x and SO_2 in a spray-type scrubber has potential to compete with the configurations that are used today, which is dominated by combining SCR and wet SO_2 scrubbing.

9
Further Work

This chapter overviews how this work could be continued and developed. There are three main points that are of great interest that are presented below.

pH Control
The scrubber system in open loop can benefit from a more rigorous pH control using an alkali, instead of an excessive amount of seawater, in terms of dimensioning and amounts of seawater used. The SO_2/NO_2 interactions have shown to be very pH dependent, and therefore a further investigation into the effects of pH control on the absorption of both NO_2 and SO_2 using an alkali is interesting.

Cost Analysis
This work lacks a cost analysis that determines if the proposed optimisation has a cost advantage over the previous configuration. The cost analysis involves construction cost, as well as operational cost such as: cost of oxidising agent and the cost benefit of reducing the liquid flow rate. A overall cost analysis could conclude if scrubbing SO_2/NO_2 is advantageous over a SCR unit or burning LNG.

Other
There are a few topics that could further develop the work. One is implementation of a holding tank, after the RateSep scrubber, in the closed loop system, in a form of a tank reactor. This could play an important role in further increasing the formation of HADS in the liquid phase, which could improve the absorption of SO_2 in closed loop. An attempt to do this was made in this work, but due to the high amounts of liquid out of the RateSep model, compositions of S(IV) and nitrogen compounds were low, which led to convergence issues.
The RateSep scrubber is a packed scrubber, where empirical data is used to calculate, for example, mass transfer rates. There is therefore many uncertainties in the validation model, and the question that arises is if the RateSep simulation behaves similarly to the Yara Marine Technology scrubber system. However, RateSep provides the alternative of overriding the empirical data and the mass transfer calculations, and inserting own calculations. This could be time consuming, but could result in a more accurate validation model.

Bibliography

[1] The Global Facilitation Partnership for Transportation and Trade, *Maritime Transport and Port Operations,*, 2015.

[2] Andreasen, A.* and Mayer, S. *Use of Seawater Scrubbing for SO2 Removal from Marine Engine Exhaust Gas*. Energy Fuels, 2007, 21 (6), pp 3274–3279

[3] Corbett. J.J., Fischbeck P.S., and Pandis S.N. *Global nitrogen and sulfur emissions inventories for oceangoing ships.* 1999, J. Geoph. Res. 104: 3457 –3470.

[4] Behrends, B., Liebezeit G. *Reducing SO2 and NOX emissions from Ships by a seawater scrubber.* Research Centre Terramare. Wilhelmshaven, Germany, 2003.

[5] International Maritime Organisation. *Prevention of air pollution from ships.* Retrieved 2016-01-18

[6] Yara Marine Technology. *Legislation.* Retrieved 2016-01-18

[7] Lloyd's Register Marine. *Understanding exhaust gas treatment systems*, 2015 Retrieved 2016-01-18

[8] DNV GL. *Upcoming environmental regulations for emissions to air – IMO NOx Tier III.* Retrieved 2016-01-18

[9] Lloyd's Register Marine. *Your options for emission compliance*, 2015 Retrieved 2016-01-18

[10] Ajdari S., Normann F., Andersson K., Johnsson F. *Modeling the Nitrogen and Sulfur Chemistry in Pressurized Flue Gas Systems*, Industrial and Chemical Engineering Research, 2015, 54 (4), 1216-1227.

[11] Andersson, K. Brynolf, S., Lindgren, F., Wilewska-Bien, M. *Shipping and the Environment.* SpringerNature, Gothenburg, 2016.

[12] PureteQ *Maritime Turbo Scrubber.* Retrieved: 2016-06-20.

[13] WÄRTSILÄ *Wärtsila Inline Scrubber System.* Available: `http://www.wartsila.com/products/marine-oil-gas/exhaust-gas-cleaning/sox-abatement/scrubber-system-designs` Retrieved: 2016-06-20.

[14] CSNOx *Ecospec.* Available: `http://www.ecospec.com/onshore-csnox` Retrieved: 2016-06-20.

[15] International Maritime Organisation. *Nitrogen Oxides (NOx) – Regulation 13.* Retrieved 2016-01-18

[16] A.A. Basfar, O.I. Fageeha, N. Kunnummal *Electron beam flue gas treatment (EBFGT) technology for simultaneous removal of SO2 and NOx from combustion of liquid fuels.* Fuel, Vol 87(8-9), 1446-1452

[17] Tsung-Wen C., Hsin C. *Removal of SO2 and NO from Flue Gas by Wet Scrubbing Using an Aqueous NaClO2 Solution*, Journal of Hazardous Materials, 01/2010; 80(1-3):43-57.

[18] IEA Clean Coal Centre *Advances in multi-pollutant control*. No 13/15, November 2013.

[19] Carvalho, M. *Combustion Technology for a Clean Environment*. CRC Press, 2002.

[20] Niessen, R.,W,. *Combustion and Incineration Processes: Applications in Environmental Engineering*. CRC Press, 2010.

[21] Eimer, D., *Gas Treating : Absorption Theory and Practice*. Somerset, NJ, USA: Wiley, 2014. Accessed March 5, 2016. ProQuest ebrary.

[22] M. A. Siddiqi, J. Krissmann, P. Peters-Gerth, M. Luckas, and K. Lucas *Spectrophotometric measurement of the vapour-liquid equilibria of (sulphur dioxide+water)*. J. Chem. Thermodynamics 1996, 28, 685–700

[23] Ajdari S., Normann F., Andersson K., and Johnsson F. *Reduced Mechanism for Nitrogen and Sulfur Chemistry in Pressurized Flue Gas Systems*. Ind. Eng. Chem. Res. 2016

[24] Whitman, W. D, *A Preliminary Experimental Confirmation of The Two-Film Theory of Gas Absorption*. Chemical and Metallurgical Engineering, Vol. 29, No. 4, 1923.

[25] MAN BW Diesel A/S *Emission Control MAN BW Two-stroke Diesel Engines*. Copenhagen, Denmark. 9/1/04.

[26] Onda K., Takeucht H., Okumoto Y. *Mass Transfer Coefficients Between Gas and Liquid Phases in Packed Columns*. Journal of Chemical Engineering of Japan, Vol. 1 (1968) No. 1 P 56-62

[27] Feron, P. *Absorption-Based Post-Combustion Capture of Carbon Dioxide*. Woodhead Publishing, 2016

[28] Schwartz S.E, White W. H. *Solubility equilibria of the nitrogen oxides and oxyacids in dilute aqueous solution*. Adv. Environ. Sci. Eng., 1981, 4

[29] Noorman, S., Gallucci, F., Annaland, M., van, S., Kuipers, H. J. A. M. *Experimental investigation of a CuO/Al2O3 oxygen carrier for chemical-looping combustion*. Ind. Eng. Chem. Res. 2010, 49, 9720– 9728

[30] Park, J. Y.,Lee, Y. N. *Solubility and decomposition kinetics of nitrous acid in aqueous solution*. J. Phys. Chem., 1988, 92, 6294-6302

[31] Clifton, C. L., Altstein, N., Huie, R. E. *Rate-constant for the reaction of NO2 with sulfur(IV) over the pH range 5.3-13*. Environ. Sci. Technol., 1988, 22, 586-589

[32] Zhenqi N., Yincheng G., Qing Z., and Wenyi L. *Experimental Studies and Rate-Based Process Simulations of CO2 Absorption with Aqueous Ammonia Solutions*. Industrial Engineering Chemistry Research 2012 51 (14), 5309-5319

A

Appendix 1

A.1 Contact Surface in Spray Scrubber

$$Volume\ of\ a\ sphere = V_{sphere} = \frac{4}{3}\pi(D/2)^3\ \ [m^2] \tag{A.1}$$

$$Volume\ of\ water\ in\ inscrubber = \frac{V_{water}}{V_{scrubber}} = 1 - \varepsilon\ \ [m^3] \tag{A.2}$$

$$Surface\ of\ a\ sphere = S_{sphere} = 4\pi(D/2)^2\ \ [m^2] \tag{A.3}$$

In order to calculate the surface area, we need to know the total amount of particles in a volume unit

$$N_{particles} = \frac{1-\varepsilon}{V_{sphere}} \tag{A.4}$$

The total surface area can be calculated to:

$$a = N_{particles} S_{sphere} = \frac{6(1-\varepsilon)}{D}\ \ [m^2/m^3] \tag{A.5}$$

A.2 Validation

Table A.1: Data set from the open loop operational mode used to further validate the RateSep open loop model.

	Liquid Feed [kg/s]	Exhaust Gas Feed [kg/s]	SO_2 ppmv (inlet:outlet)
1	142.5	18.1	864:57
2	152.8	13.2	843:9
3	163.3	18.5	864:36
4	177.5	19	843:24
5	179.1	16	843:9
6	179.7	15.8	843:9
7	180.3	16.1	843:8
8	181.4	17.7	843:20
9	181.4	17.7	843:14
10	184.7	18.5	843:20